

THE ANATOMY OF A LARGE DEVONIAN BLACK SHALE GAS FIELD

by

Jane Negus-de Wys

West Virginia University
Department of Geology and Geography
Morgantown, West Virginia 26506

570

LIST OF FIGURES

	<u>Page</u>
Figure 1. Geological provinces and orogenic trend lines (after Muehlberger, <u>et al.</u> , 1967).	169
Figure 2. Field location relative to the epicontinental shelf (after Price in Lafferty, 1941), the New York-Alabama Lineament (King and Zietz, 1978), Grenville metamorphic front (Bass, 1960), Cincinnati Arch, and oil and gas occurrence.	170
Figure 3. Three dimensional interpretation of basement structure after Shumaker (1977).	171
Figure 4. Sequential structural development.	172
Figure 5. Evidence of major development of the Rome Trough in Cambrian time (after Dever, <u>et al.</u> , (1977).	173
Figure 6. Structure on top of the Ohio shale (after Provo, 1977).	174
Figure 7. Isopach map of total Ohio shale.	175
Figure 8. Stratigraphic cross section E'-E, north to south through the southern end of the field, showing log traces of natural radioactivity from the gamma ray logs.	176
Figure 9. Stratigraphic cross section B-B', southwest to northeast through the field center, showing log traces of natural radioactivity from the formation density logs.	1 7 7
Figure 10. Stratigraphic cross section K'-K, north to south through the northern end of the field, showing traces of natural radioactivity from the gamma ray logs.	178
Figure 11. Lithology cross section A-A'.	179
Figure 12. Map showing iso-value lines of percent green clay-shale of total shale sequence.	180
Figure 13. Isopach map of highly organic black mud-shale (in feet).	181
Figure 14. Map showing iso-value lines of percent gray clay- to mud-shale of total sequence.	182
Figure 15. Map showing iso-value lines of percent organic brown silty mud-shale of total shale sequence.	183
Figure 16. Structure on top of the Fire Clay coal (after McFarlan, 1943).	184

LIST OF FIGURES - continued

	<u>Page</u>
Figure 17. Cartoon comparison of depositional and present attitudes of Fire Clay coal and black shales.	185
Figure 18. Map of observed frequency of fracture horizons in wells studied.	186
Figure 19. Rock shale pressure decline of 200# contour from 1935-1951 (after Hunter and Young, 1953).	187
Figure 20. Data points used by Griffith (1976).	188
Figure 21. Histogram of all wells used in computer-mapping (4138).	189
Figure 22. Histogram tail of Figure 21 showing highest value 19 wells.	190
Figure 23. Contours of density of high producing wells (after Griffith, 1976).	191
Figure 24. Hand-contoured map of open flow data with three contour levels, using 4750 wells.	192
Figure 25. Trends of high open flow data taken from Figure 24.	193
Figure 26. Pattern resulting from connecting all wells with $\geq .5$ MMcf/day where not contra indicated.	194
Figure 27. Pattern of open flow basic fracture band trends from Figure 26.	195
Figure 28. Comparison of similar cross sections.	196

THE ANATOMY OF A LARGE DEVONIAN BLACK SHALE GAS FIELD

Jane Negus-deWys

West Virginia University, Morgantown, West Virginia, U.S.A.

ABSTRACT

The gas occurrence and production from approximately 5000 wells is compared with lithofacies changes and other stratigraphic features, structural development, and fracture occurrence in the largest Upper Devonian black shale gas field in the Appalachian Basin, North America. Lithology studies suggest complex depositional history of craton-derived organic, muds-intertonguing with distal, deltaic, fine gray silts and green mud-shale. Two bentonite zones indicate volcanic activity prior to more intense basinal subsidence. Fracture frequency is contoured over the field area. Structural development is related to continental plate rifting and collision. Three major structural trends persist from the Pre-Cambrian; north-south, northeast-southwest, and east-west. Production studies of open flow data from 5000 wells in this 3000 square mile area include computer-drawn contours, trend-surface analysis pattern interpretation, and polar plot trends of high production. A series of radiating high fracture of fault zones is suggested. Gas recovery appears to be governed by fractures intercepting siltier zones in thick sequences of highly organic black shale in the area of greatest complexity of intertonguing. The relative importance of the different parameters is discussed and assessed, using statistical correlations. The methods of analysis and model of field conditions may be applicable to other shale basins.

Introduction

The "Big Sandy" gas field is located in eastern Kentucky on the western flank of the central Appalachian Mountains, at the junction of two orogenic trend directions. Figure 1 shows the study area in relationship to the Precambrian orogenic provinces in North America. The area studied covers about 3000 square miles.

The gas in the eastern Kentucky field is produced primarily from fractures in the Upper Devonian black shale of the Ohio Shale sequence. The field is situated at the distal terminus of deltaic sedimentation originating to the east and northeast. These fine clastics intertongue complexly with black organic muds primarily derived from the west and north. Figure 2 shows the field location in eastern Kentucky relative to the epicontinental shelf and the aeromagnetic anomaly of King and Zietz. The areas of oil and gas accumulation lie directly to the northwest of this anomaly, which also shows up in gravity data.

The basement in the field area is dominated by a trough reaching a depth of -16,000 feet in the northeast, and which trends in a north easterly direction across the northern edge of the field. At nearly 90 degrees to this trough, known as the Rome Trough, the Floyd County Channel extends northward to, and perhaps into, the trough. The channel is flanked on the east and west by slight uplifts. Figure 3

shows a three-dimensional block diagram of these basement features. Figure 4 shows the sequential development of structural features. The area of the Rome Trough shows continued activity up to the present time, but with the major development occurring in Cambrian time.

Evidence for the major development of this trough is seen in the thickened sequence of Cambrian sediments caused by growth of the asymmetrical graben at that time (Figure 5).

Structure and Stratigraphy

Present structure on top of the producing horizon, the Ohio Shale, shows a north-south trending uplift which broadens to the south, southeast (Figure 6). This structure, known as the Paint Creek Uplift, appears to exert a major control on gas' accumulation in the field as will be shown later.

Ohio Shale sediments thicken to the east (Figure 7) with a N-S strike to the nearly parallel isopachous lines.

Cross sections drawn from gamma-ray logs in the field indicate a relatively constant thickness of sediments in the southwest (Figure 8) which increases in thickness from 300' to 900' across the field to the northeast (Figure 9). Complex intertonguing of silty zones with organic zones is suggested by the gamma-ray log signature. The lower Huron, the basal shale in the sequence, shows especially high natural radioactivity. Figure 10 shows the relatively constant thickness at the northeastern end of the field, but thicker than the section in the southwest.

Cross sections developed from lithology studies on well cuttings confirm the complex intertonguing of black, gray, green, and brown silty shales. The highly organic black mud shale is thicker in the center of the field; the green and gray shales are more dominant to the east and northeast (Figure 11).

Bentonite zones below the base of the Ohio Shale and at the base of the Cleveland black shale at the top of the Ohio Shale sequence are evidence of volcanic ashfalls immediately prior to thicker black shale deposition and increased basinal subsidence in the eastern and north-eastern parts of the field.

Studies of relative percentages of the different shale types suggest the green clay shale source may be to the northeast (Figure 12). The area of thickest black shale is located off the nose of the Paint Creek Uplift (Figure 13). The gray shale which commonly contains vitrinite or woody fragments is most dominant in the southwest central portion of the field, suggesting perhaps a northwestern source (Figure 14). The brown, frequently very silty, mud-shale is lowest to the east and more dominant to the northwest, west and southwest. This silty organic shale is also suggestive of a western cratonic source.

The present structure on the Pennsylvanian Fire Clay Coal (Figure 15) indicates uplift occurring in the southeast and hinging along a NE-SW trending synclinal axis known as the eastern Kentucky syncline (Figure 16). The northern part of this syncline is part of the Rome Trough. This syncline is interrupted by the N-S trending Paint Creek Uplift, which forms a saddle or barrier between what results in a northeastern basin and southwestern basin. The tectonic movements involved in the formation of these features were probably instrumental in developing highly fractured zones related to the nose of the Paint Creek Uplift, the eastern Kentucky syncline, and the uplift to the southeast.

Thrust sheets in the southeast, i.e., Pine Mountain thrust sheet,

and the southeastern uplift are related to plate collision interactions along the continental plate margins, commencing after Devonian sedimentation.

The changes in depositional and present attitudes of the Fire Clay coal relative to the black shales indicate uplift of the black shales at the extreme NW and 'SE of the field area, but **downwarp** in the extreme NE and SW, with the hingeline for uplift **along** the eastern Kentucky **syncline** and the saddle for downwarp provided by the Paint Creek Uplift (Figure 17).

The plot of fracture frequencies based on data from **lithology** studies and core data shows the highest concentration of fractures along the central portion of the eastern Kentucky syncline and off the nose of the Paint Creek Uplift (Figure 18).

Gas Occurrence and Recovery

Pressure **decline** plots of the 200 pound isopressure contour show the contour **moving away** from the center of high production in the period plotted: 1935-1951. This is evidence of an interconnected gas reservoir in the field (Figure 19).

For a comparison of the gas isopotential (an indication of gas occurrence and production) the final open flow data from **4750 wells** were analyzed. Well distribution is shown in Figure 20.

A histogram of the open flow data shows a nearly asymptotic curve with 0.06 MMcf per day as the economical cutoff for "dry" holes (Figure 21). The tail of this histogram extends out **to > 8.6 MMcf** per day but only includes 19 wells between 2.4 and 8.6 MMcf per day (Figure 22).

Contours of high producing wells **per 25 square miles**, representing a density value of wells producing at a given rate, show the greatest concentration of higher producers centered in south-central Floyd County with a N-E trend (Figure 23). The western boundary of high production **is fairly** straight, but irregular, linear projections are apparent to the north, east and southeast.

Contouring of the open flow data results in a highly complex configuration (Figure 24), suggestive of a coalescence of many smaller-fields,...

Trends of open flow configurations plotted from Figure 24 show multidirectional trends both in low open flow and in the high open flow patterns (Figure 26), resulting in Figure 27. **These** trends suggest higher fracture zones extending in bands radiating off the **nose of** the Paint Creek Uplift and sharply cut off along a line' parallel to the eastern Kentucky syncline.

A comparison of cross sections is shown in Figure 28. The section through open flow data (#3) shows higher values over the area of structural high **on the** Paint Creek Uplift, even though the dip of the strata is only 30-50 feet per mile. Black shale lithotype is-thickest over this central area of-high production, and **greater** complexity of intertonguing of gray, green, brown, and black shales occurs in the central portion of the field.

The geochemistry cross sections which are not discussed in this paper, also show abnormalities in the central area.

Summary

In conclusion, the Big Sandy Field, which is estimated to be capable of producing 2 trillion cubic feet of gas from the present 5000 wells, represents a highly complex structural-stratigraphic gas trap. It may be considered a coalescence of many smaller fields, but in general shows the high gas concentration and recovery from fractures to be related to the interaction of southeastern uplift hinged along the eastern Kentucky syncline and abutting against, and interrupted by the Paint Creek Uplift. Thicker organic black shales and complex intertonguing with silty zones providing a "fracture facies" are undoubtedly important factors in gas recovery from the Upper Devonian black shales in the largest gas field in the Appalachian Basin.

Acknowledgement.

This research was funded under Department of Energy Contract, DE-AC21-76-MC-05194, formerly EY-76-C-05-5194, and monitored by the Morgantown Energy Technology Center, Morgantown, West Virginia, United States of America.

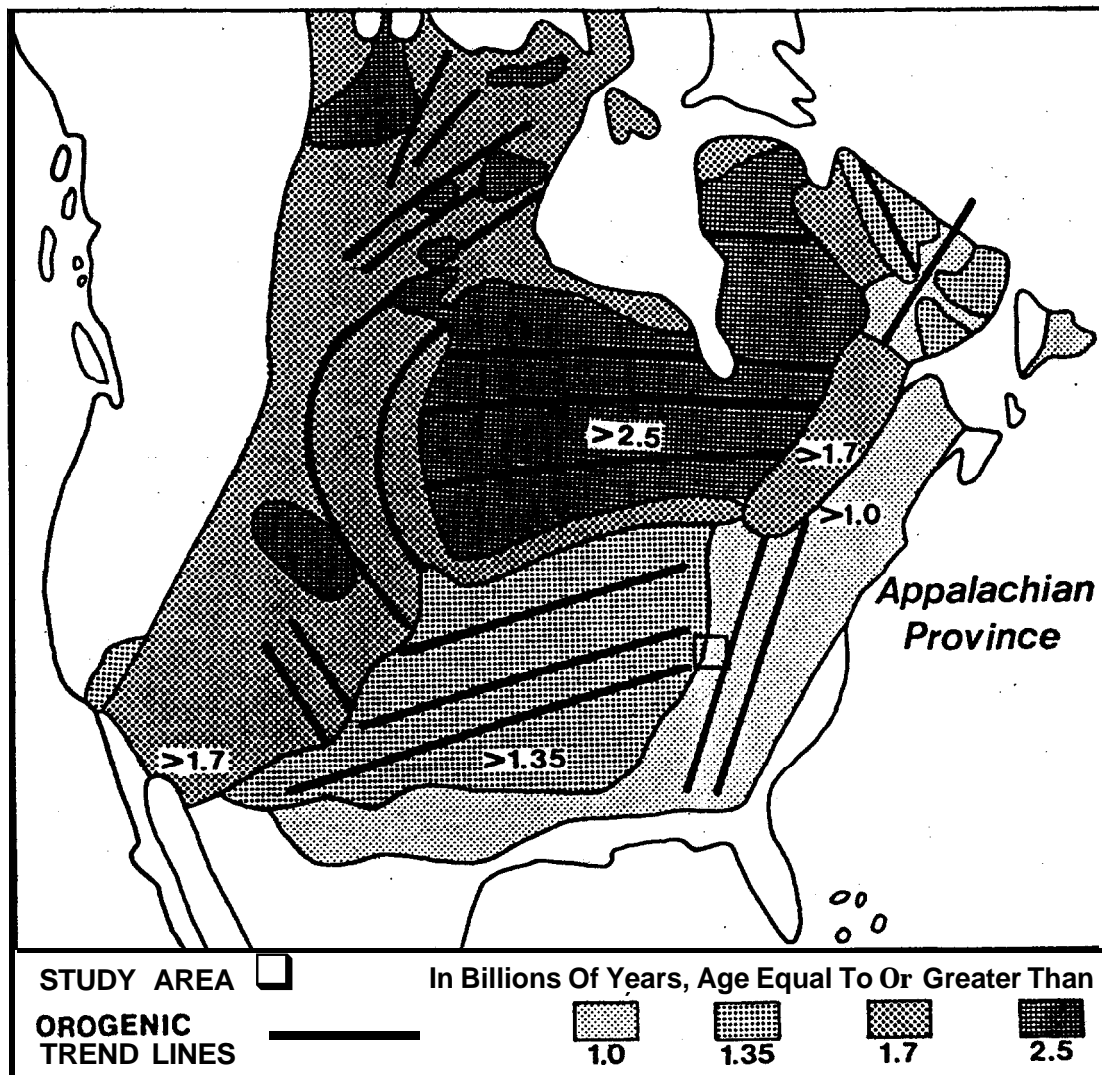


Figure 1. Geological provinces and orogenic trend lines (after Muehlberger, et al. 1967). The location of study area is shown by rectangle. Province ages are in billions of years.

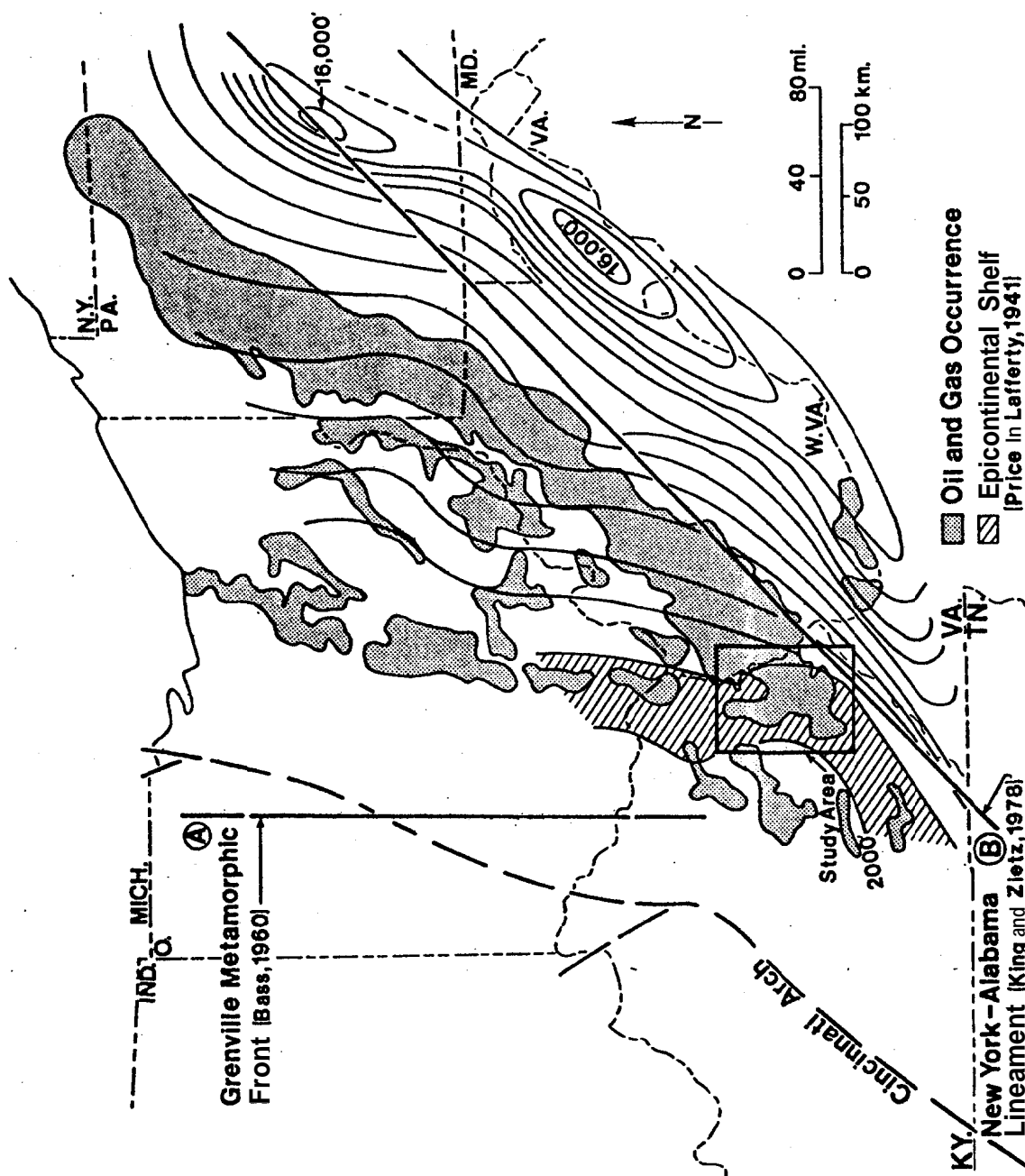


Figure 2. Field location relative to the epicontinental shelf (after Price in Lafferty, 1941), the New York-Alabama Lineament (King and Zietz, 1978), Grenville metamorphic front (Bass, 1960), Cincinnati Arch, and oil and gas occurrence. Contours are of thickness of early, Paleozoic clastics.

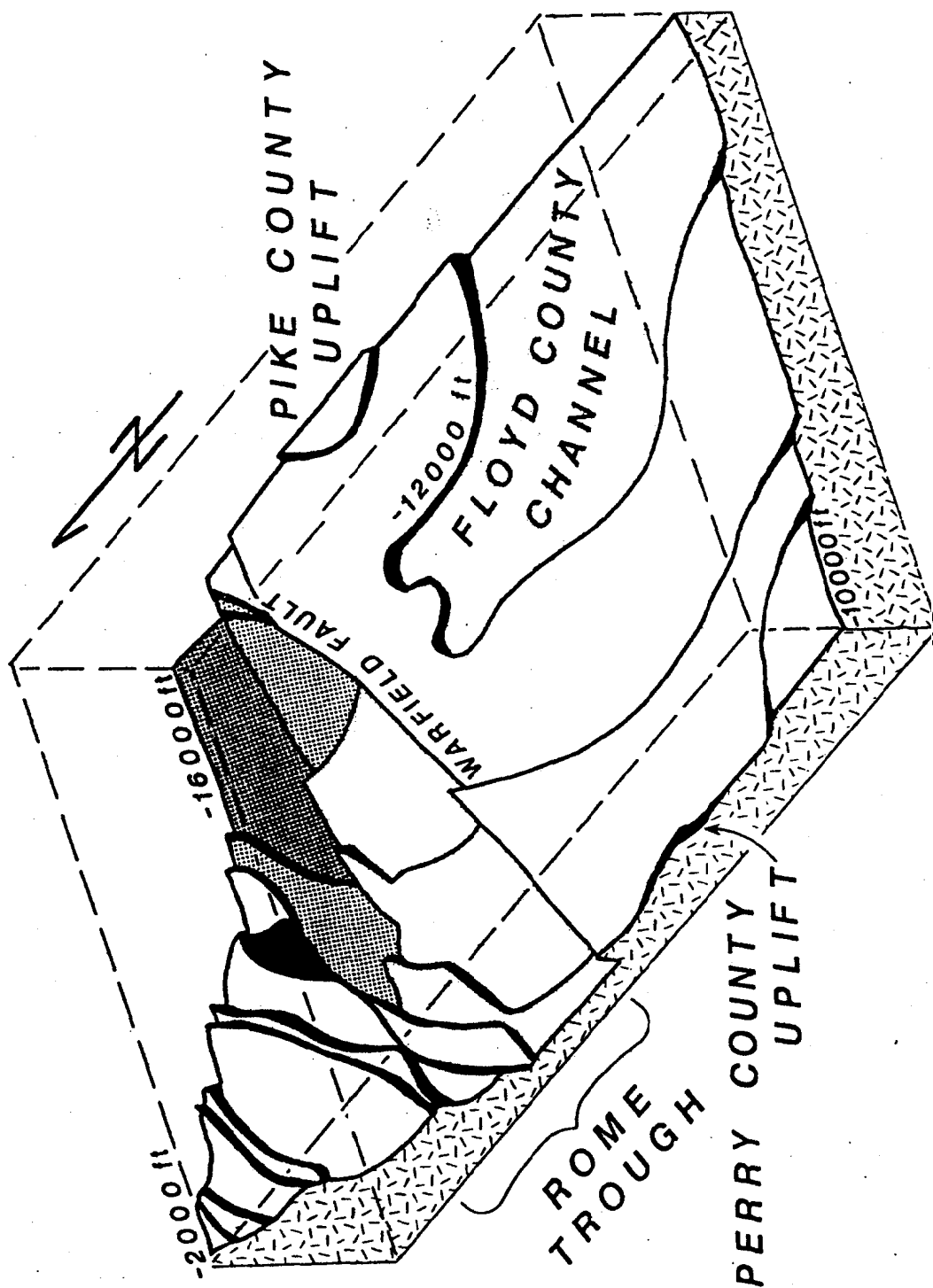


Figure 3. Three dimensional interpretation of basement structure after Shumaker (1977). Breaks are shown on contours. Actual structure would probably be smoothed out between contours except in the Rome Trough area. Note 14,000-foot difference in depth of trough in the northeast corner, when compared with 2,000-foot depth of trough margin.

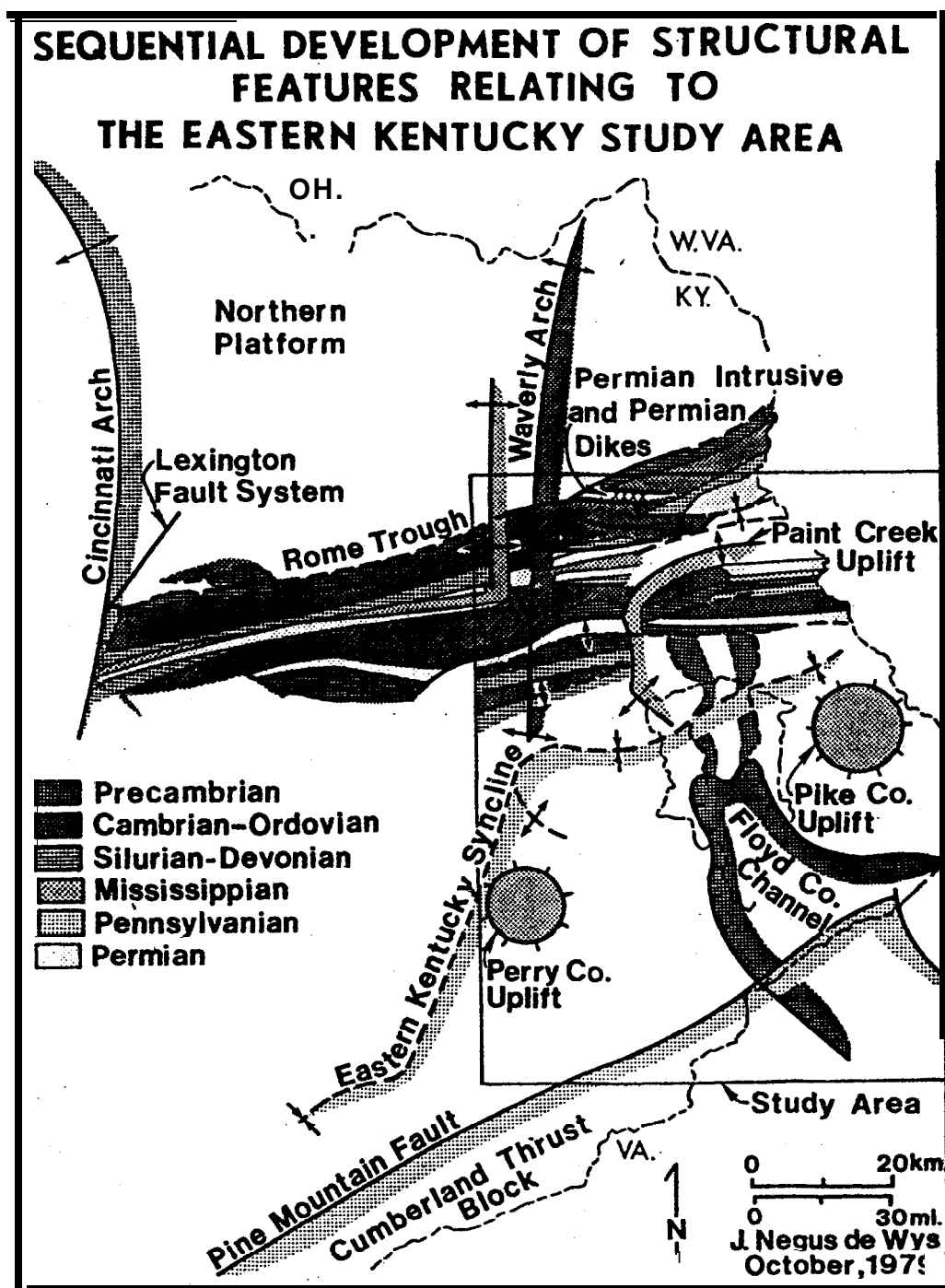


Figure 4. Sequential structural development.

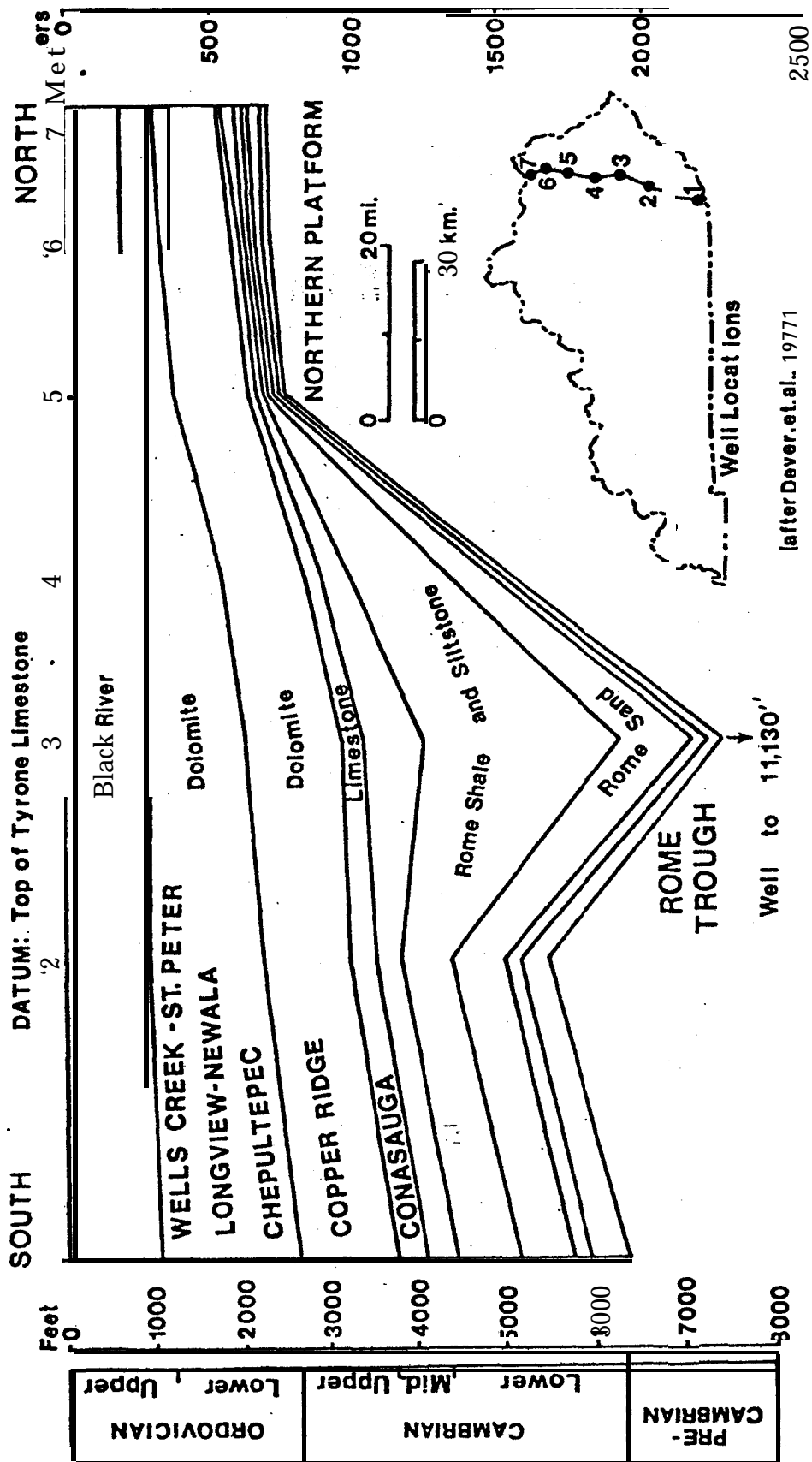


Figure 5. Evidence of major development of the Rome Trough in Cambrian time (after Dever, et al., 1977).

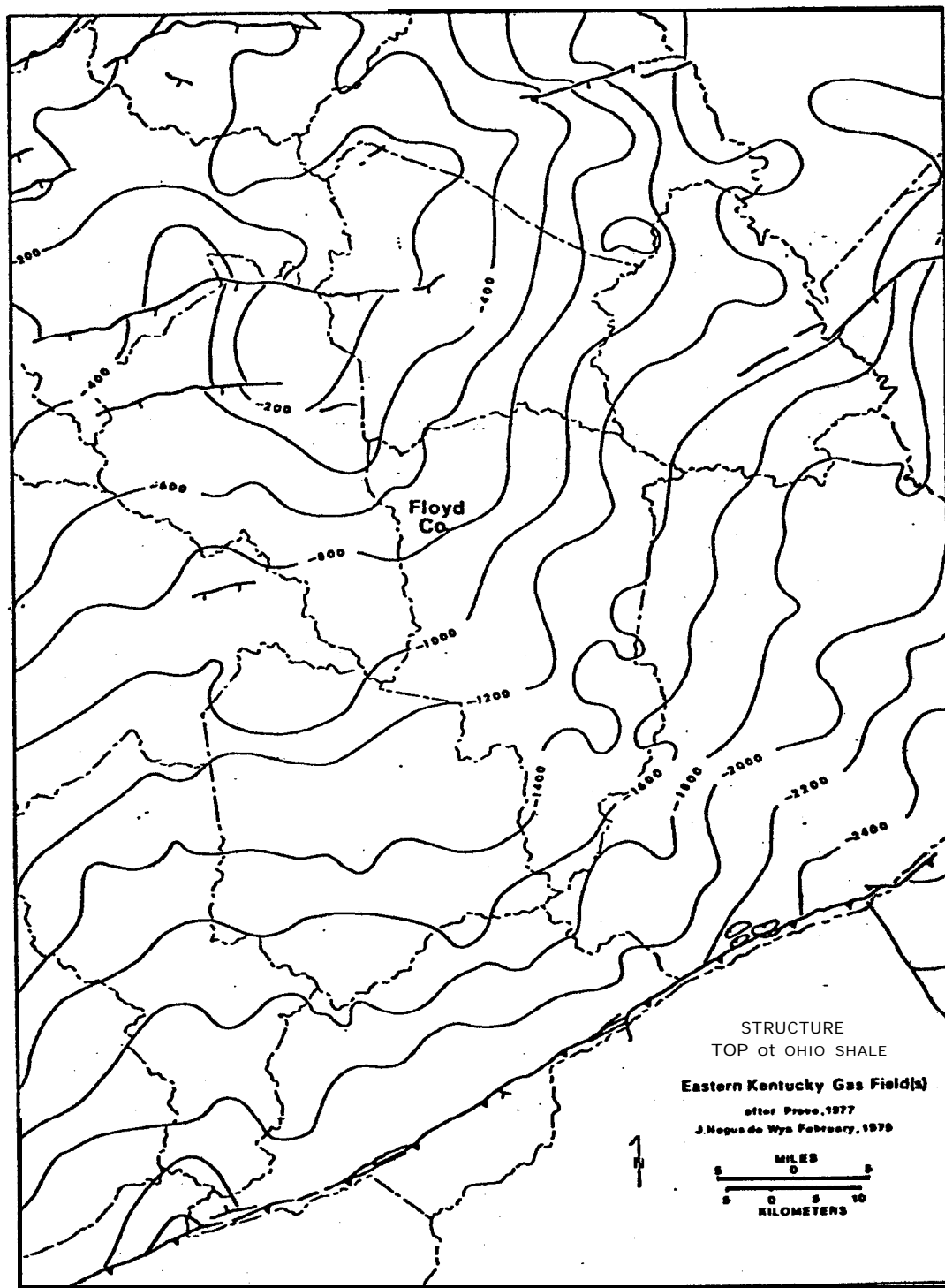
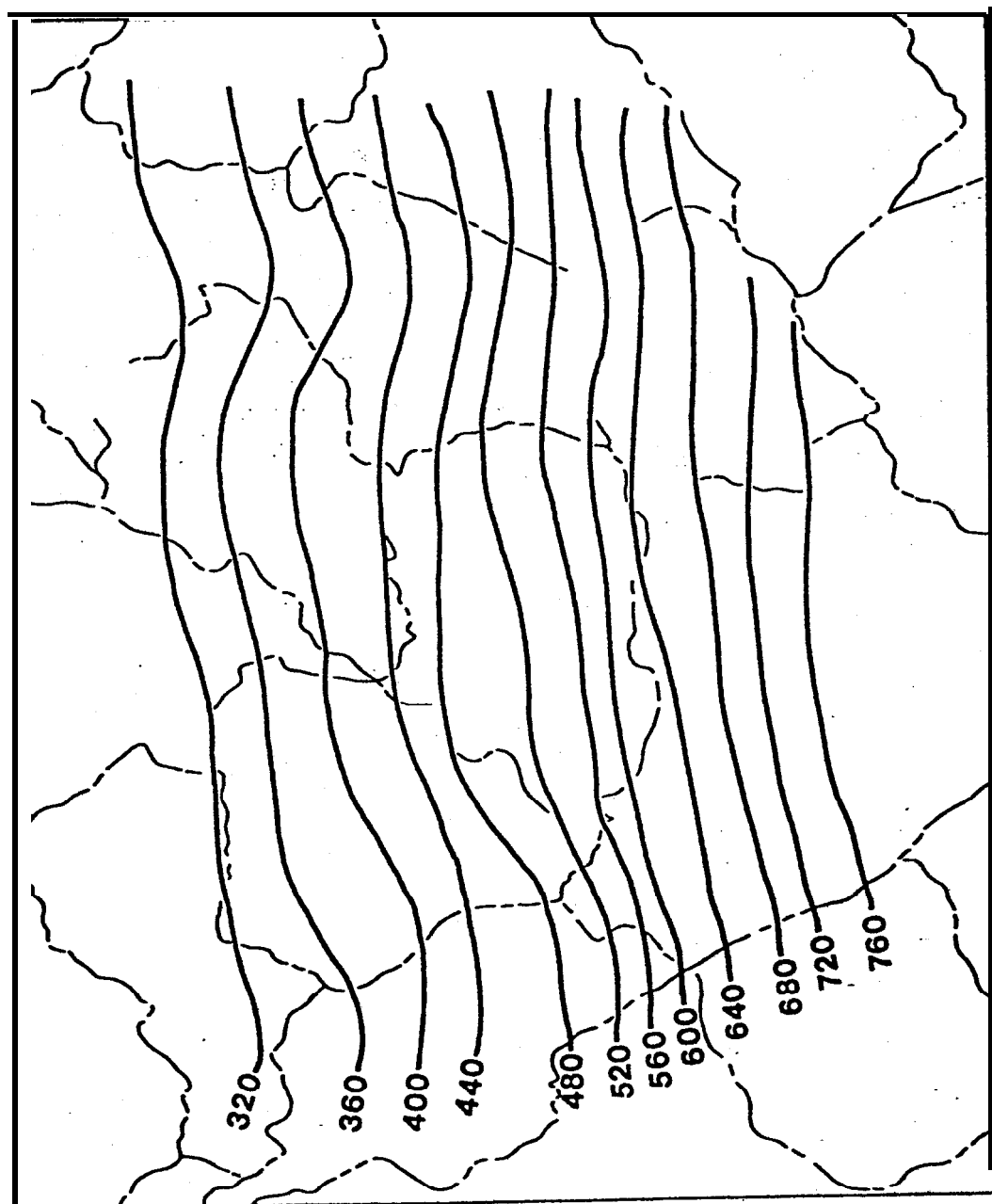


Figure 6. Structure on top of the Ohio Shale (after Provo, 1977).



Isopachs of Total Ohio Shale

deWys, 1979

Figure 7. Isopachmap of total Ohio Shale.

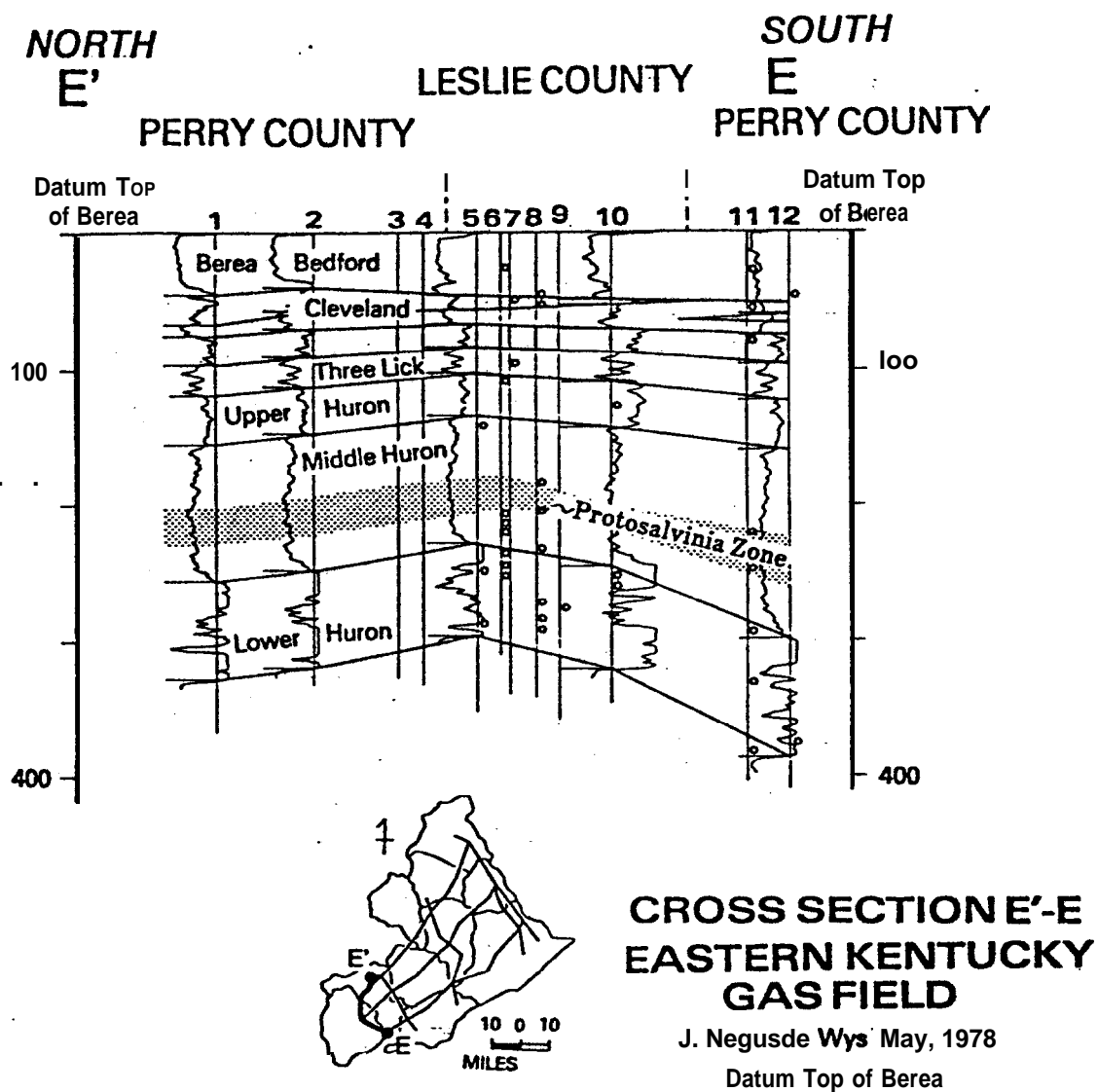


Figure 8. Stratigraphic cross section E'-E, north to south through the southern end of the field, showing log traces of natural radioactivity from the gamma ray logs. The black shale in the Cleveland is shaded gray.

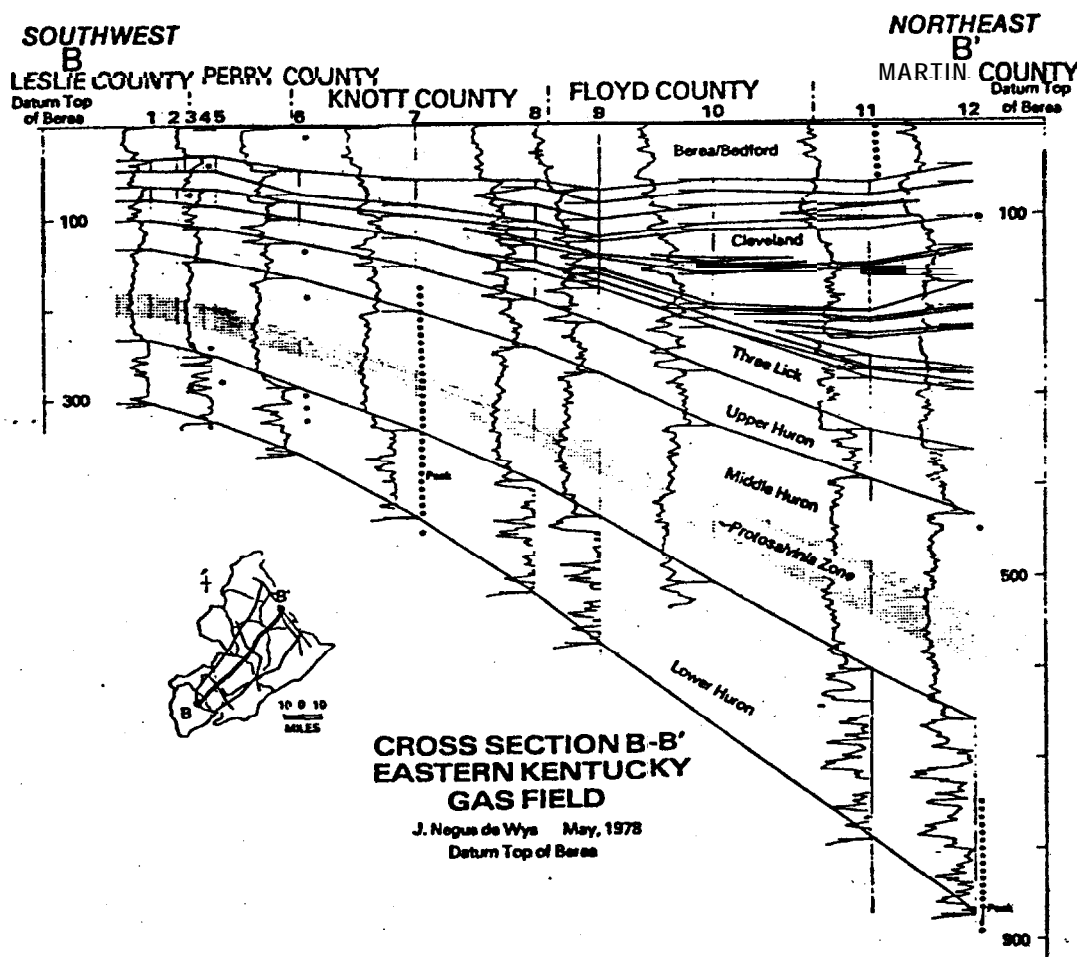


Figure 9. Stratigraphic cross section B-B', southwest to northeast through the field center, showing log traces of natural radioactivity from the formation density logs. Intertonguing of the black and gray shales in the Cleveland are usually related to the changes in natural radioactivity. The black shale in the Cleveland is shaded gray.

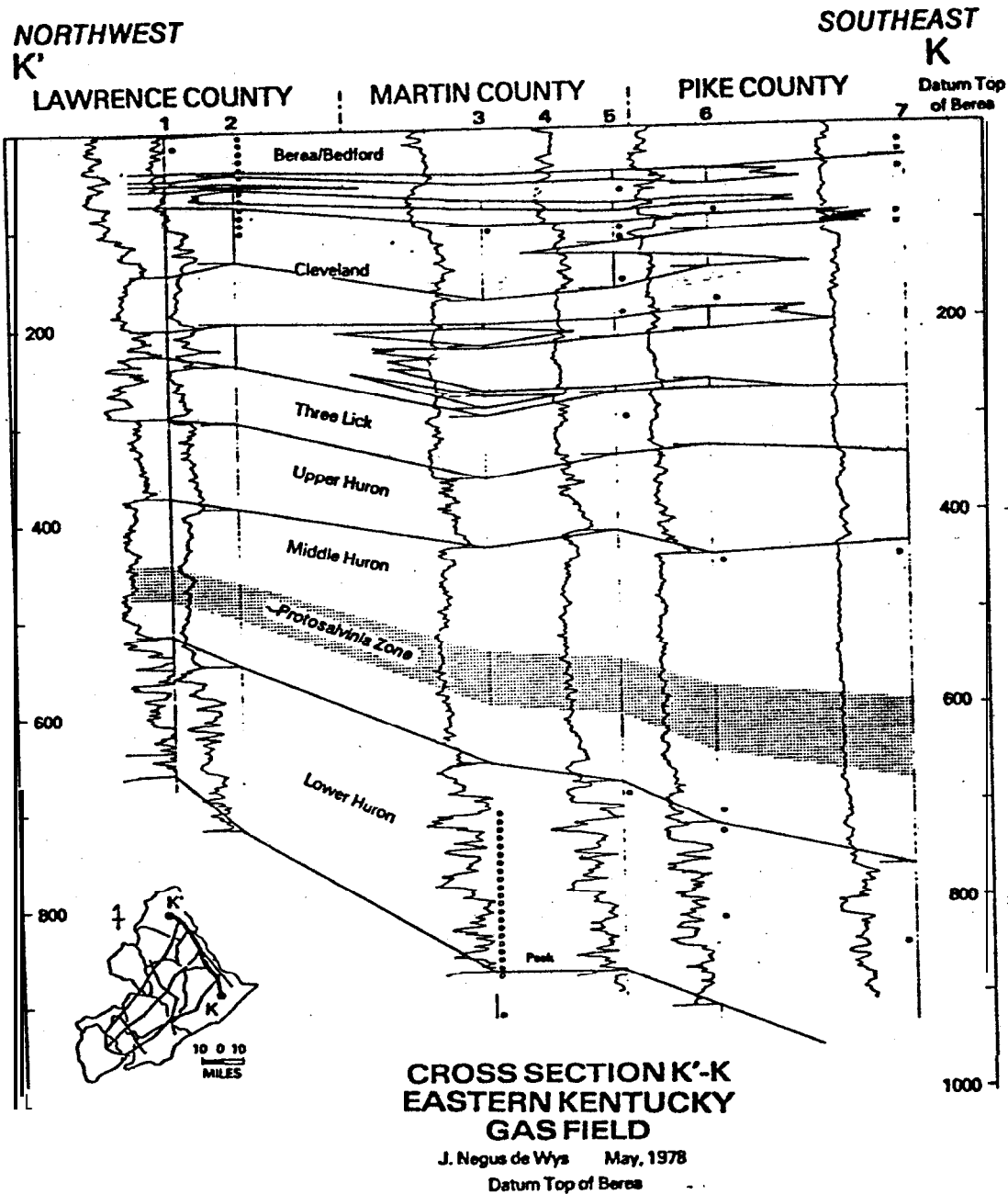


Figure 10. Stratigraphic cross section K'-K, north to south through the northern end of the field, showing traces of natural radioactivity from the gamma ray logs. The Protosalvinia zone is where the brown algae occur most commonly. It has been reported at horizons in the Three Lick down through the Lower Huron (Provo, 1977; Swager, 1978).

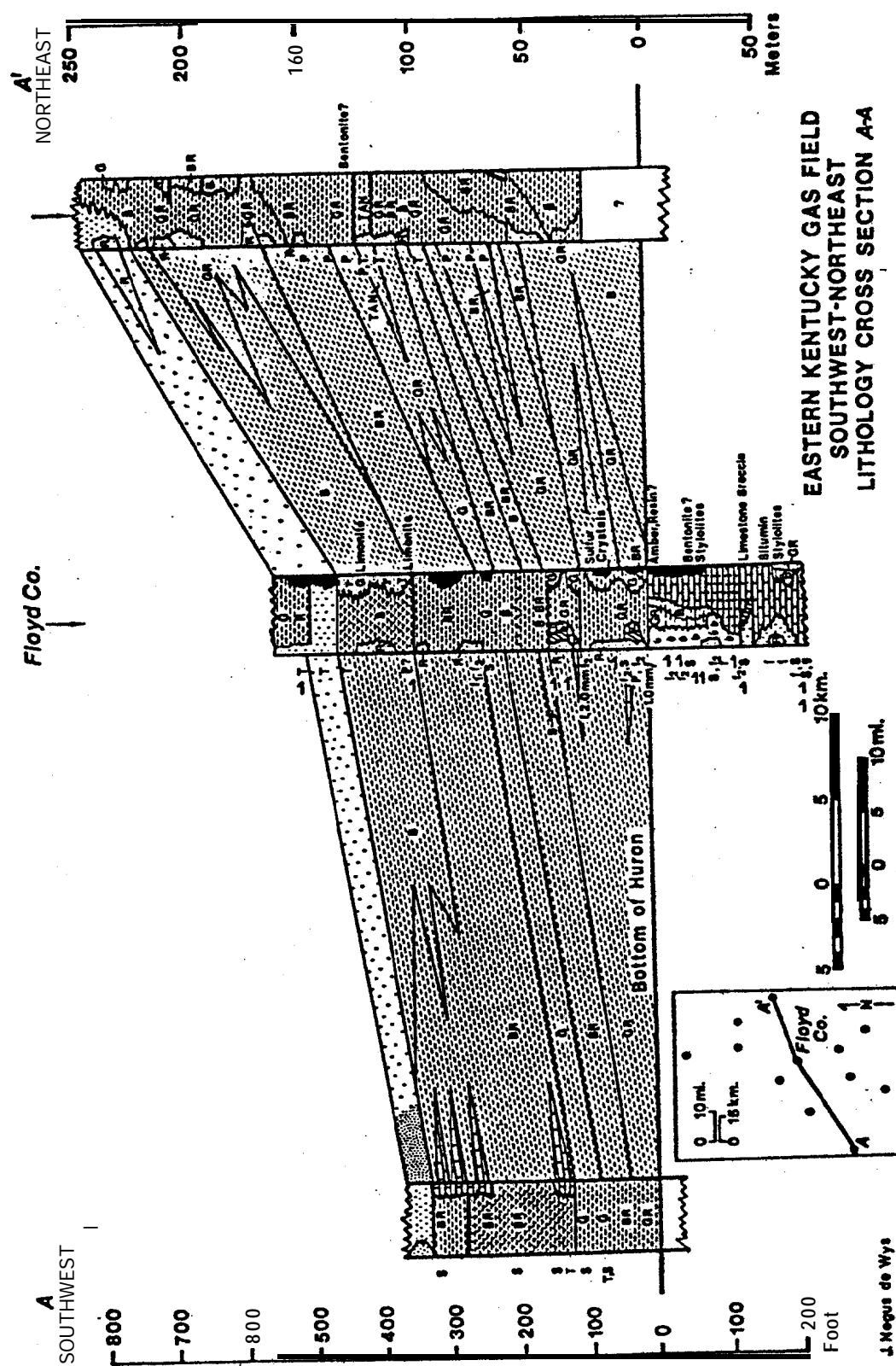


Figure Lithology cross section A-A'.

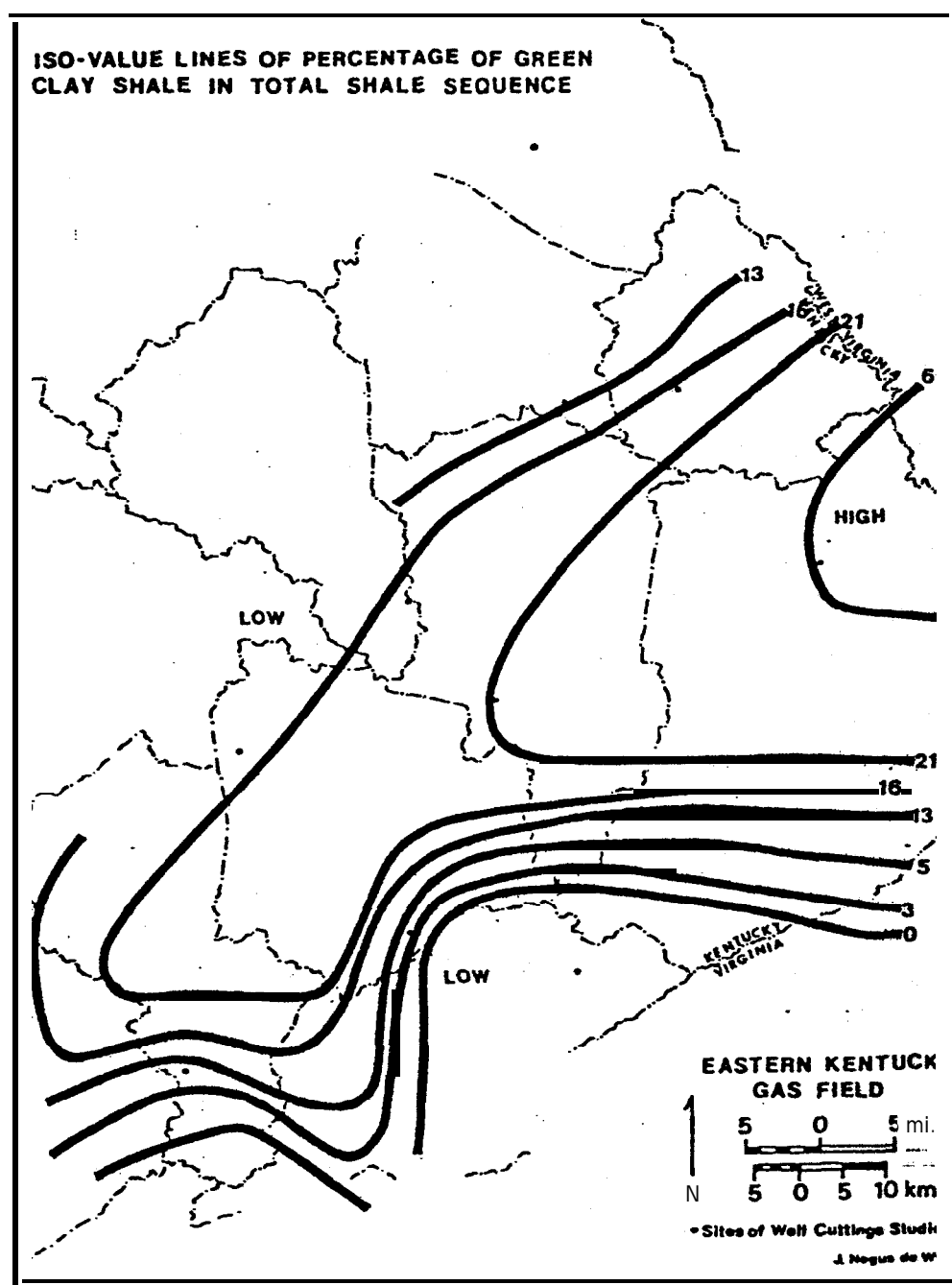


Figure 12. Map showing iso-value lines of percent green clay-shale of total shale sequence,

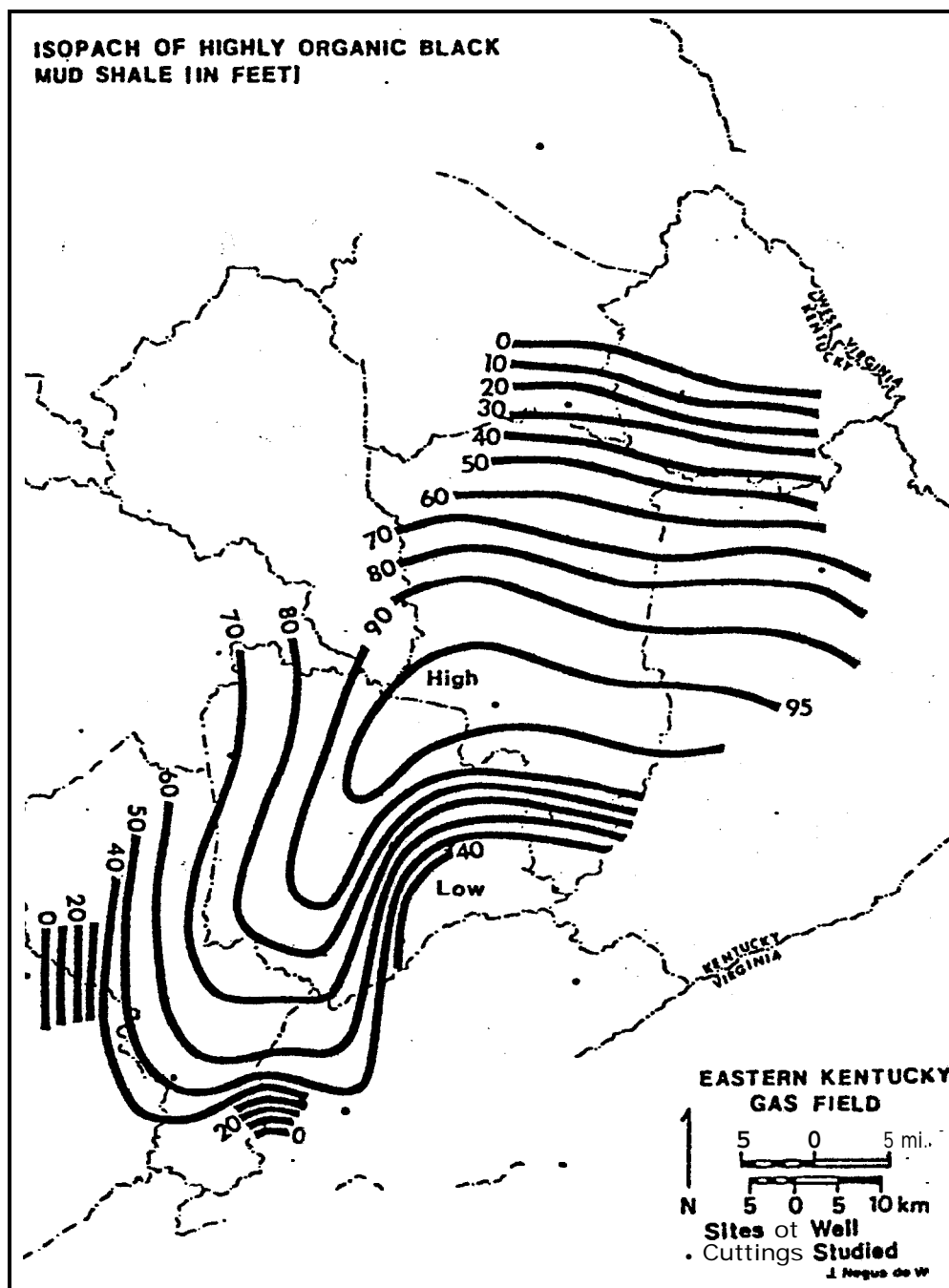


Figure 13. Isopach map of highly organic black mud-shale (in feet).

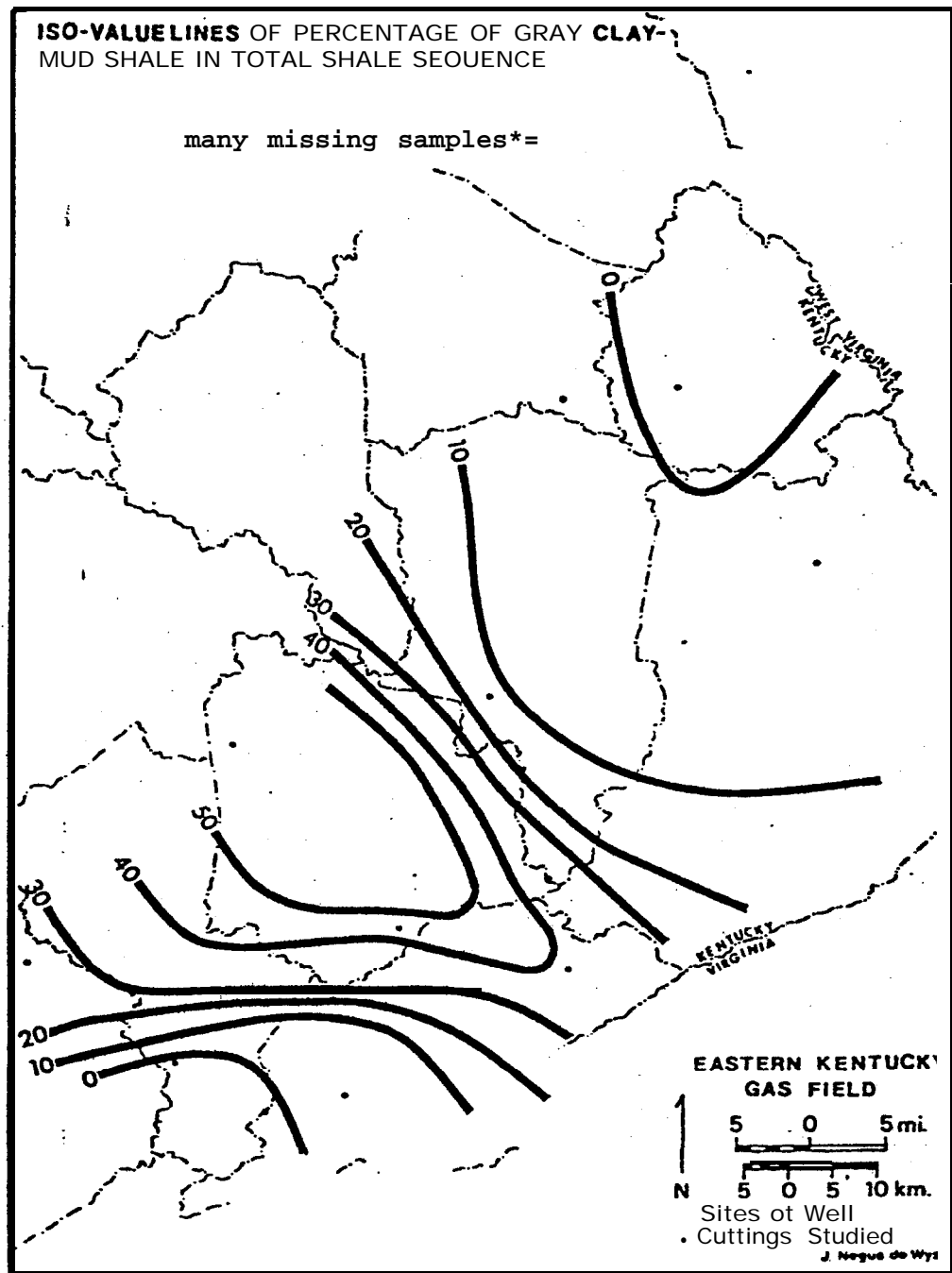


Figure '14. Map showing iso-value lines of percent gray clay- to mud-shale of total sequence.

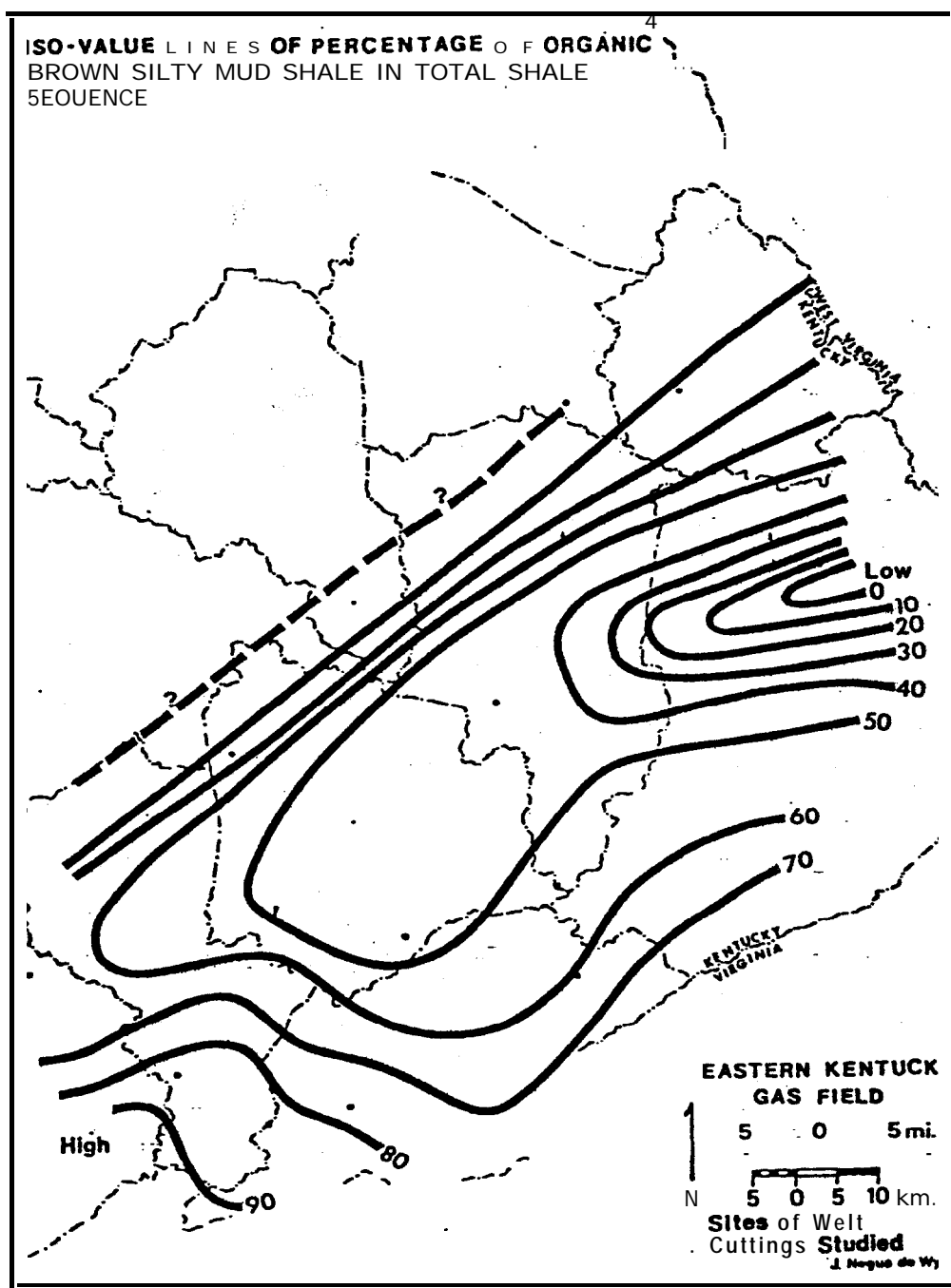


Figure 15. Map showing iso-value lines of percent organic brown silty mud-shale of total shale sequence.

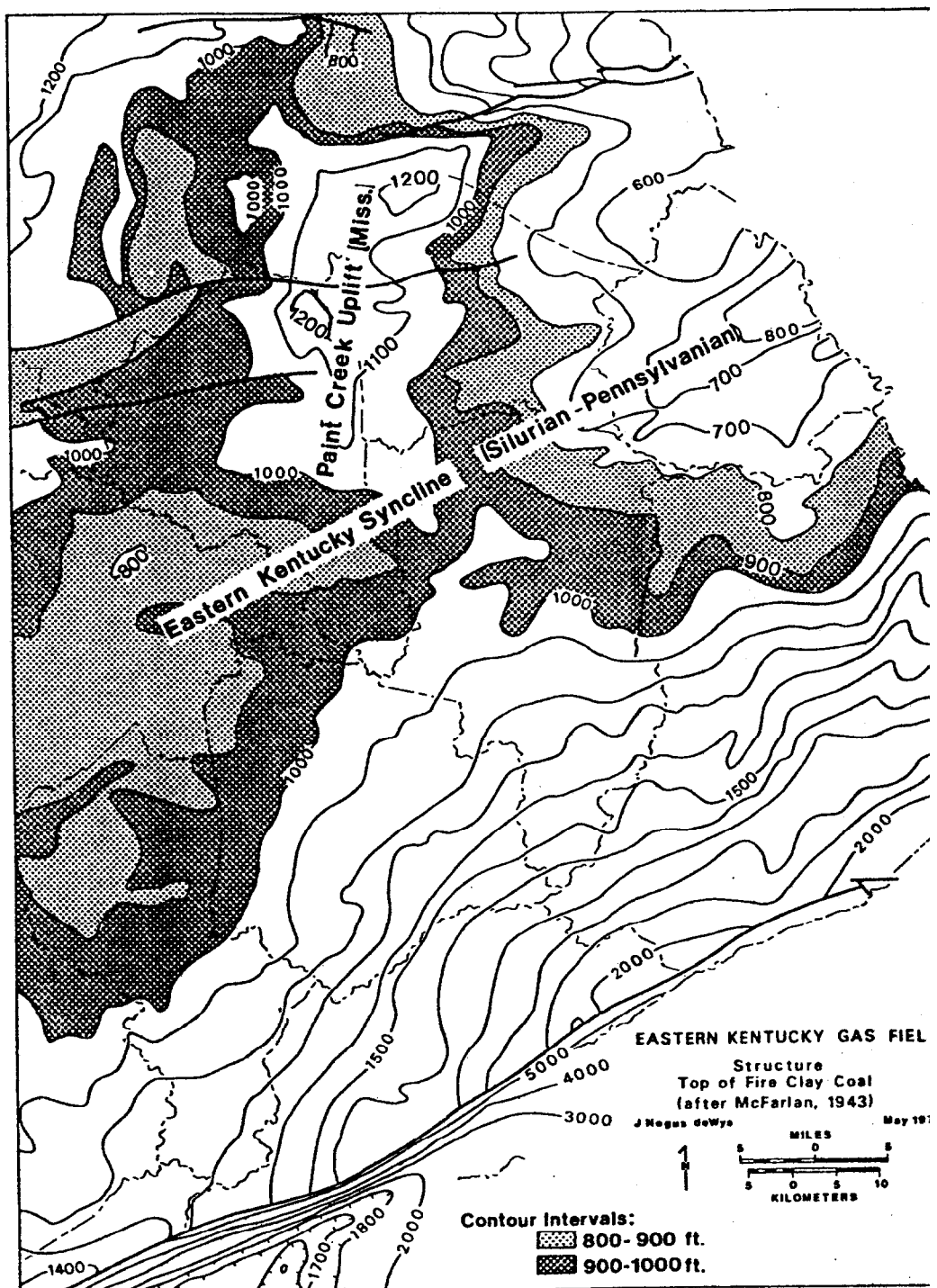


Figure 16. Structure on top of the Fire Clay coal (after McFarlan, 1943). Note: Northeast-southwest trend of syncline interrupted by the N-S trend of the Paint Creek Uplift; the northeast basin is deeper than the southwest basin; this is the area (NE) where the "Corniferous" limestone isopach suggests an early basin; and this northeastern area is suggested by geochemistry to be an area of marine tidal influence. Age of structural development is indicated in parentheses.

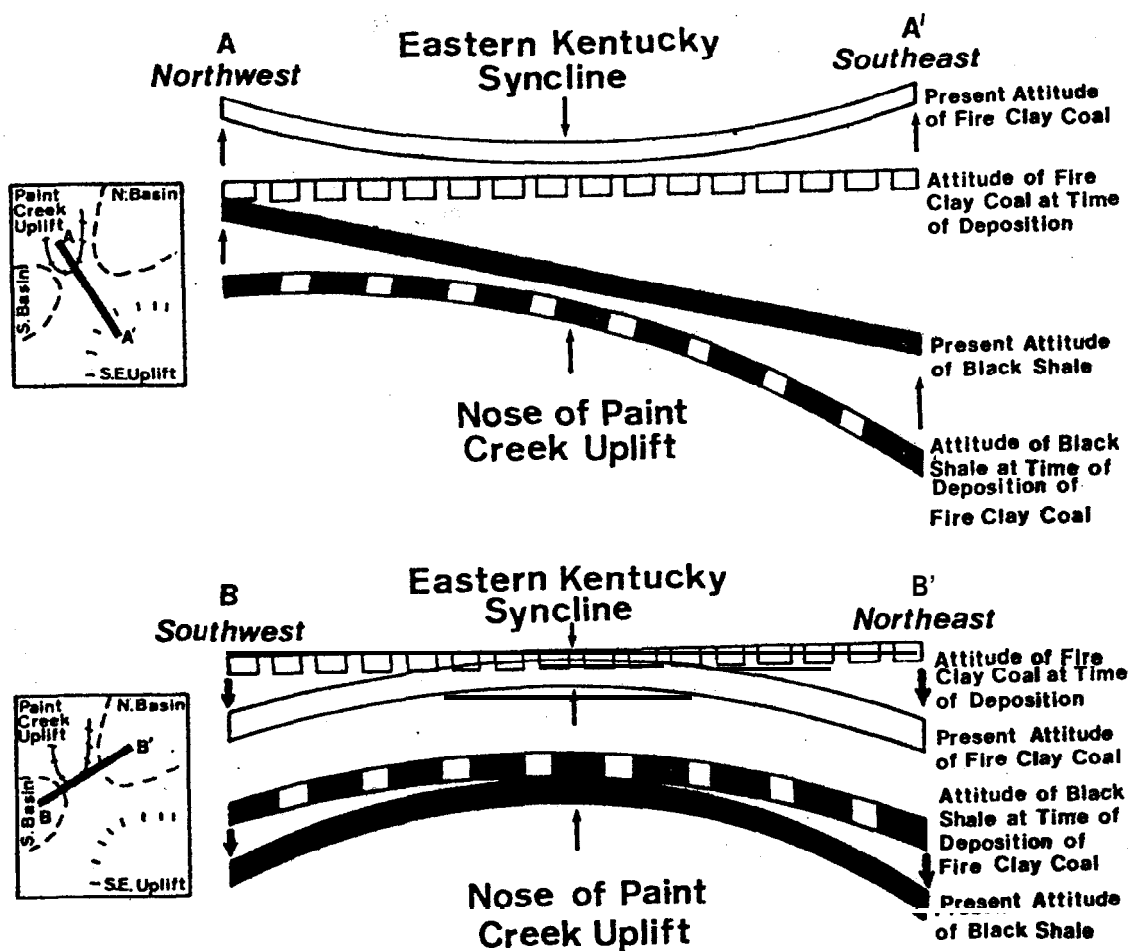


Figure 17. Cartoon comparison of depositional and present attitudes of Fire Clay coal and black shales. No scale is intended. Upper diagram after McFarlan, 1943.

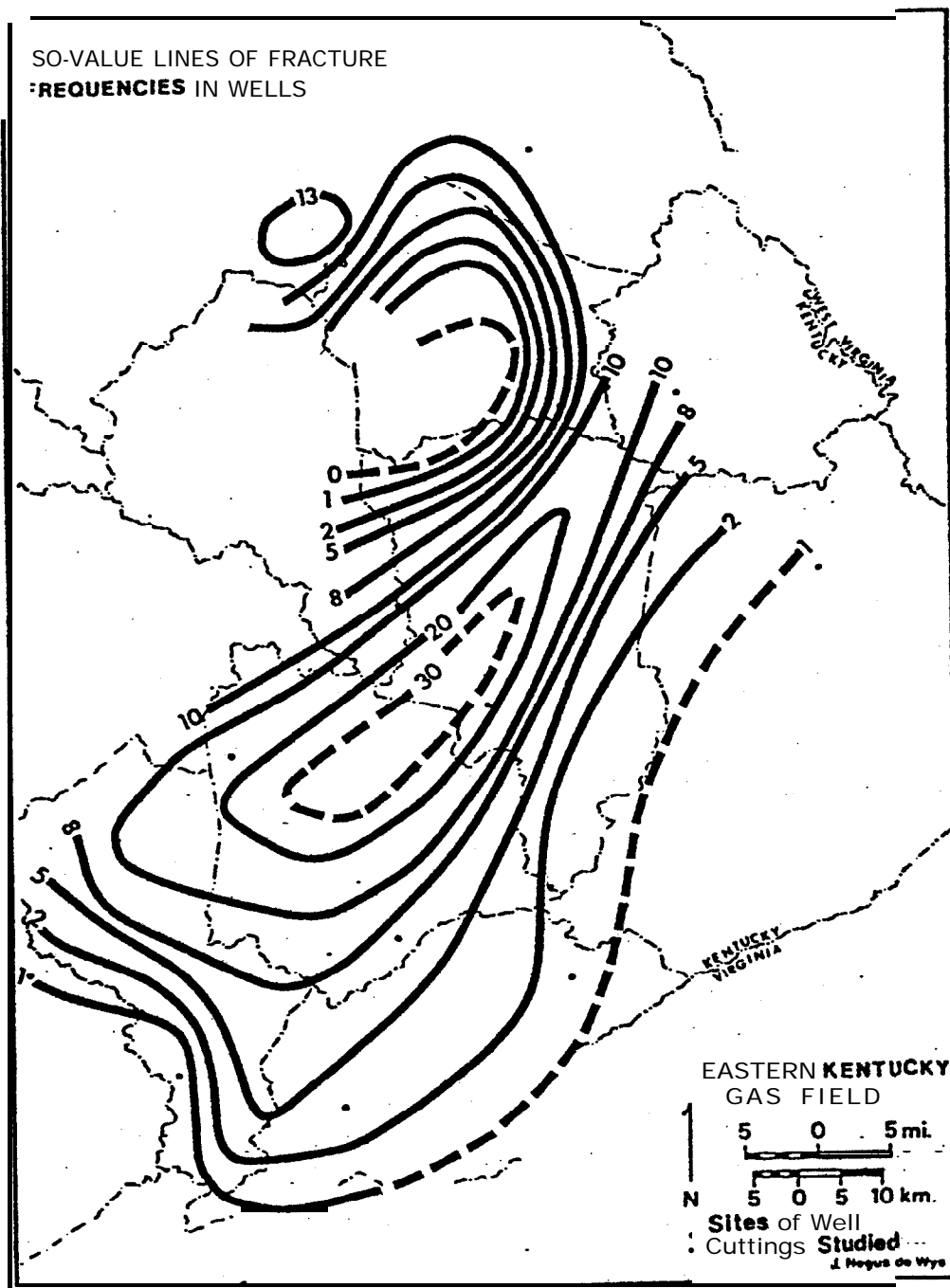


Figure 18. Map of observed frequency of fracture horizons in wells studied.

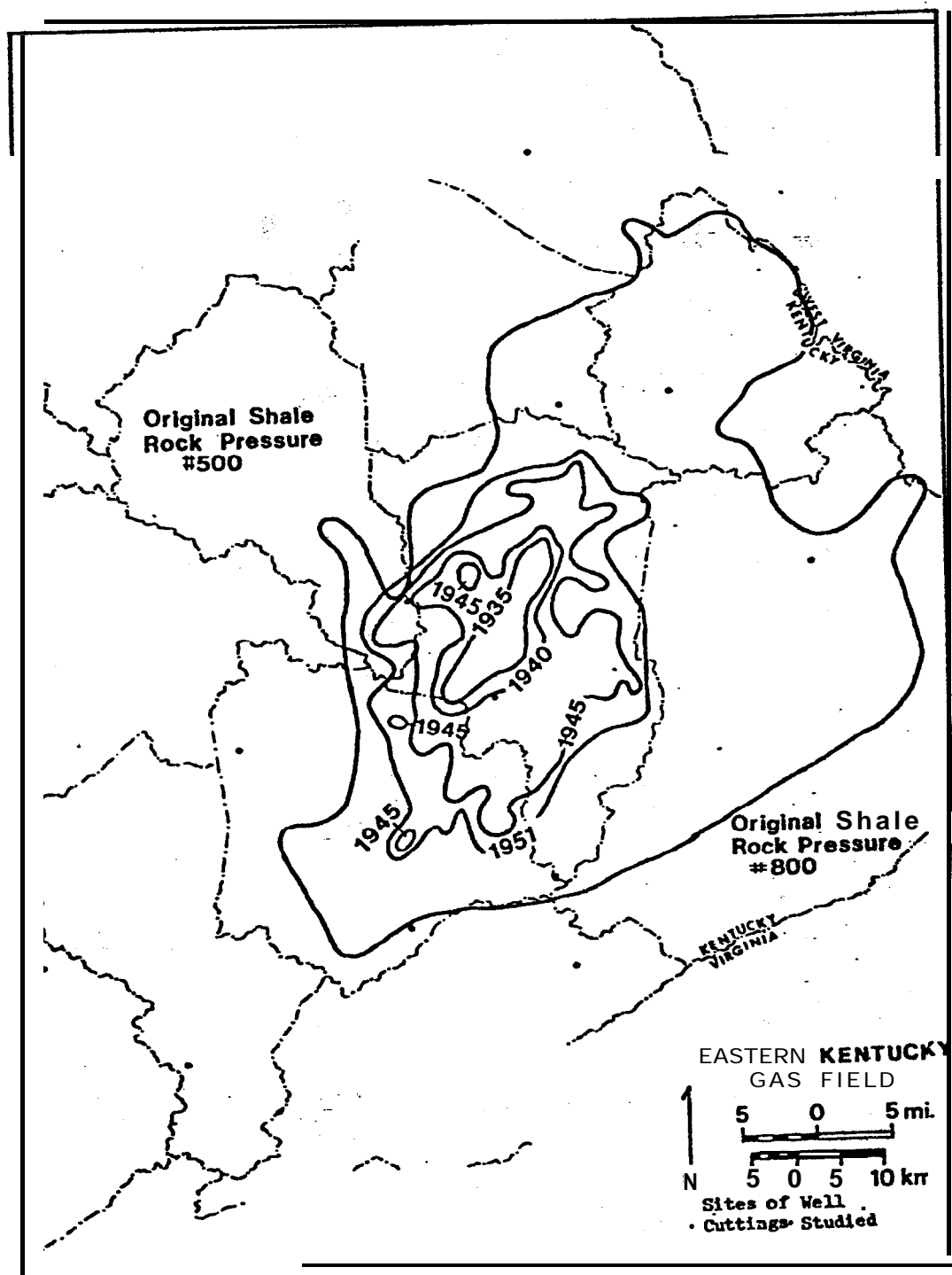


Figure 19. Rock shale pressure decline of 2008 contour from 1935-1951 (after Hunter and Young, 1953).

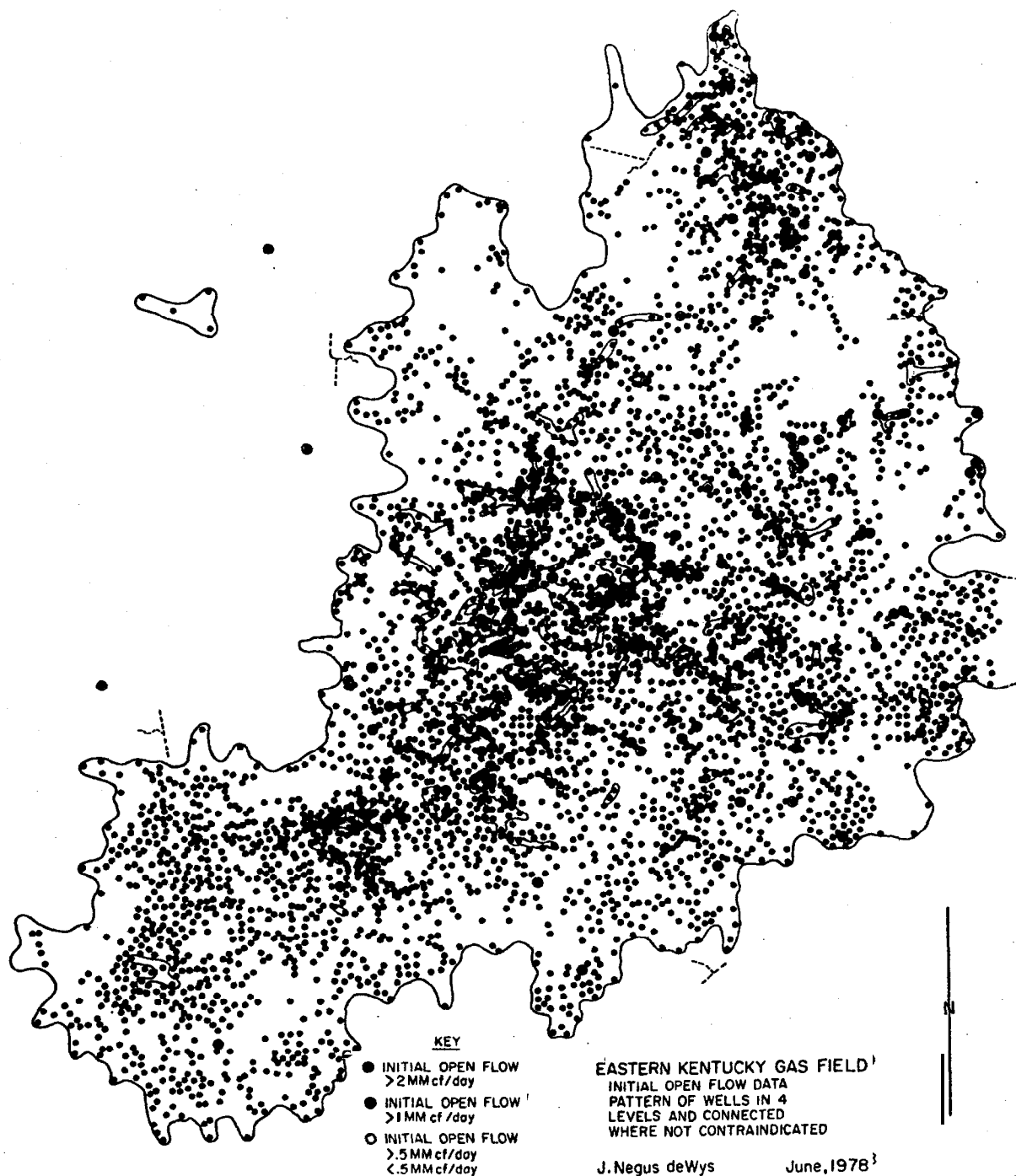


Figure 20. Data points used by Griffith (1976). Points $\geq .5$ MMcf/day are connected where not contra indicated.

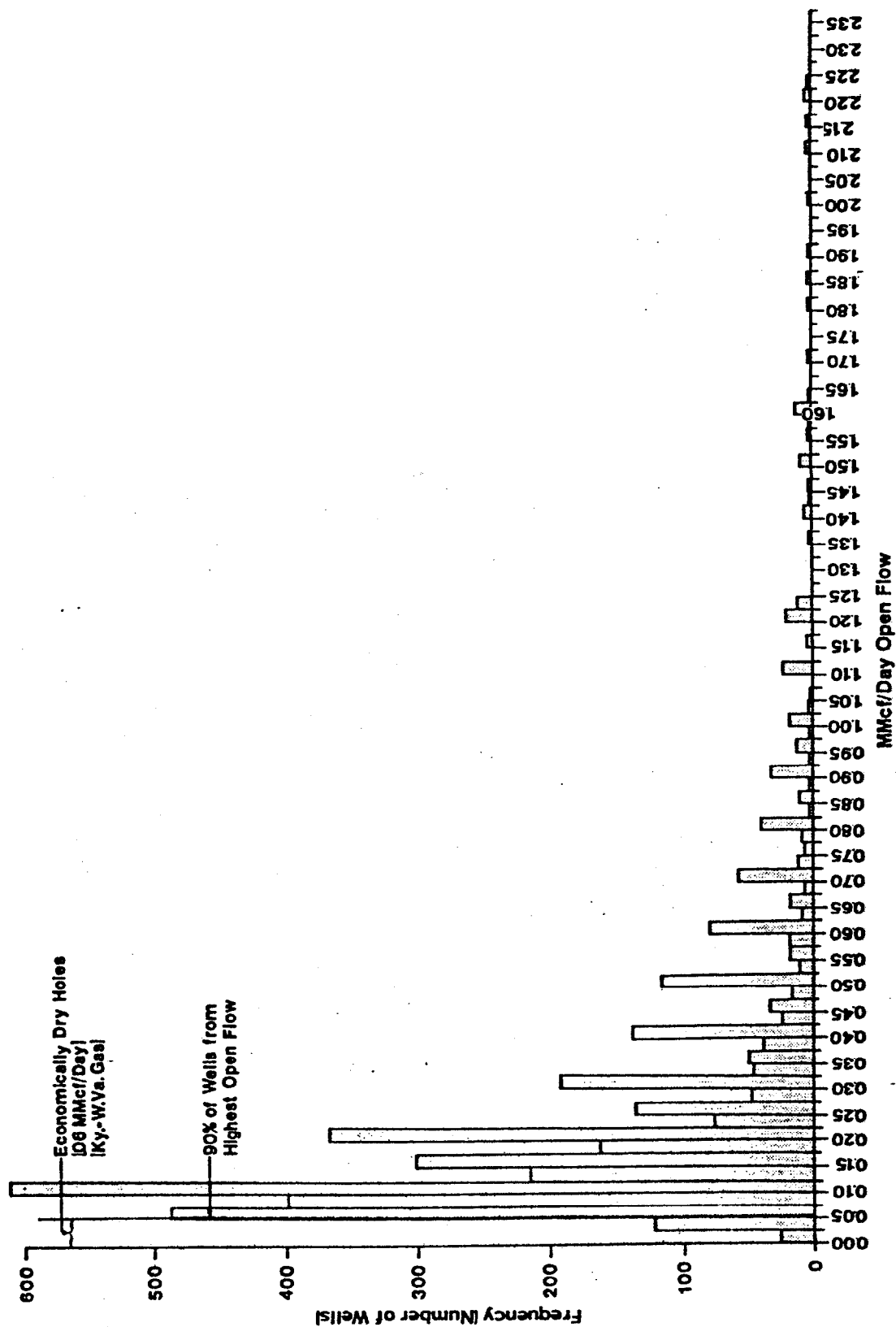


Figure 21. Histogram of all wells used in computer-mapping (4138). Figure 22 shows tail of histogram representing only 19 wells.

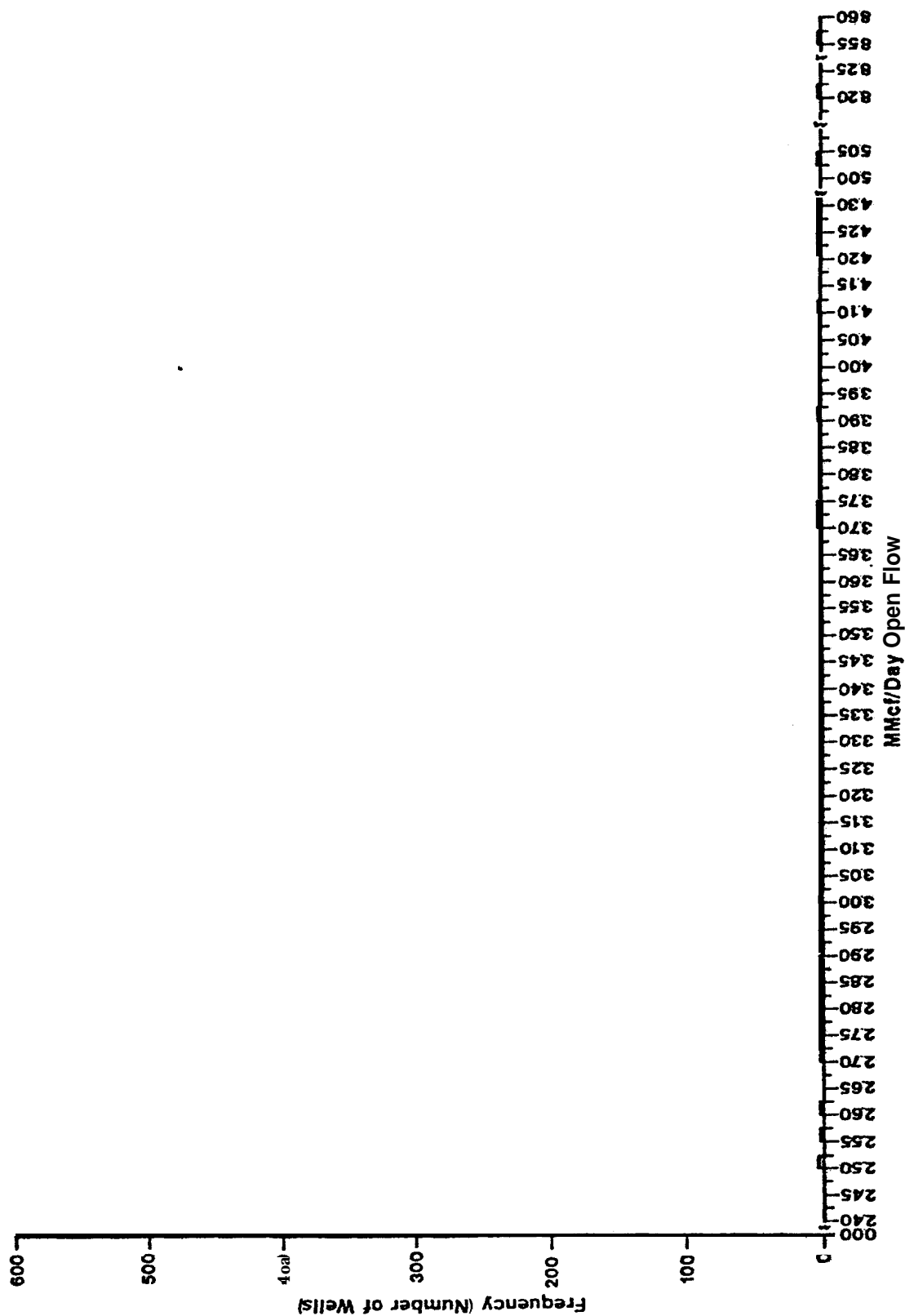
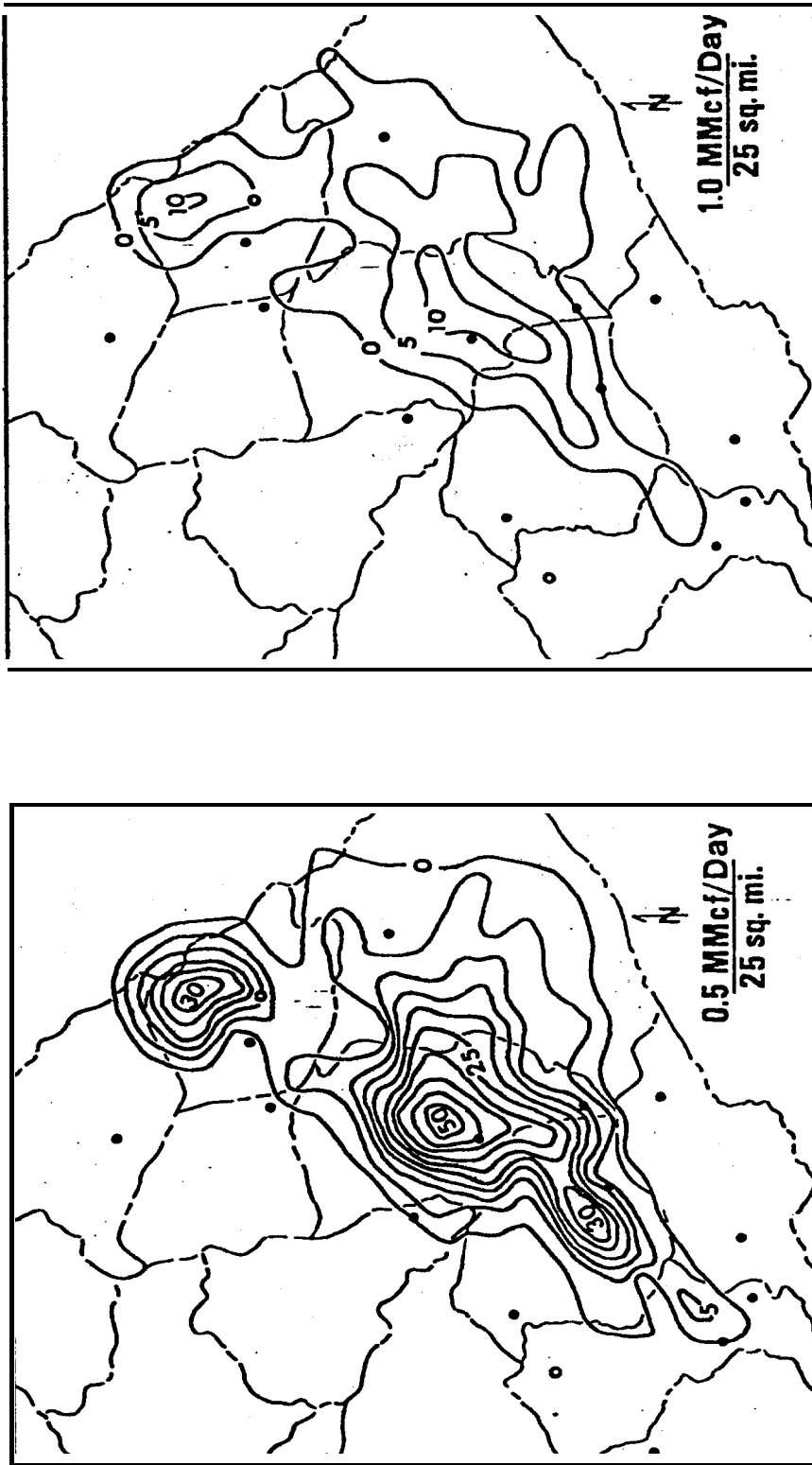


Figure 22. Histogram tail of Fig. 21 showing highest value 19 wells, Note histogram must be broken twice on the horizontal scale.



J. Negus deWys
March, 1979

Figure .23

Contours of density of high producing wells (after Griffith, 1976). Contours represent number of wells ≥ 0.5 MMcf/day/25 square miles (left) and ≥ 1 MMcf/day/25 square miles (right). These figures may be interpreted as the area of gas accumulation with recovery details smoothed out. Note pattern irregularities suggesting linear peripheral extensions.

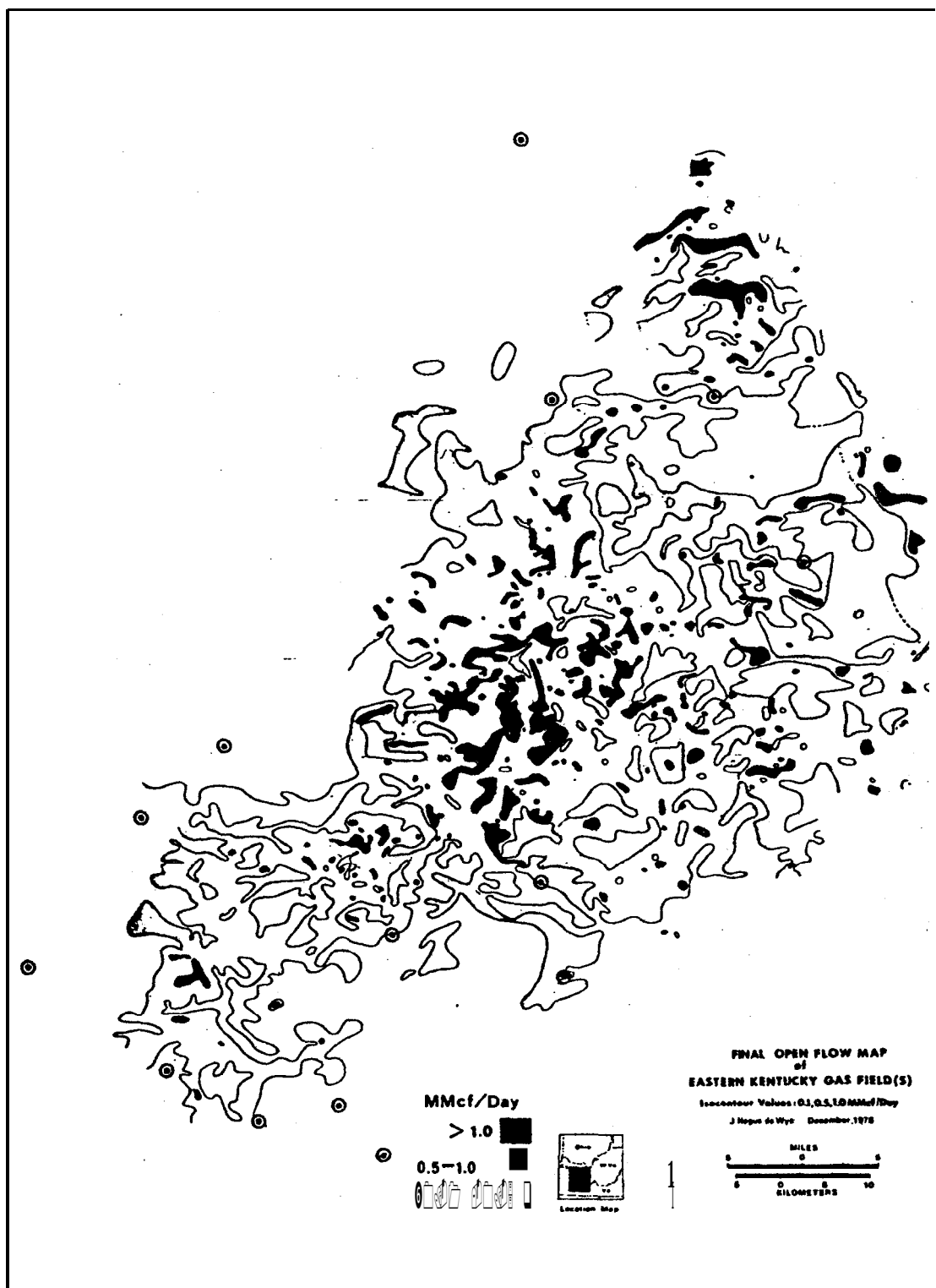


Figure 24. Hand-contoured map of open flow data with three contour levels, using 4750 wells. The highest value areas are shaded to enhance the pattern of higher open flow. Circled dots are locations of wells used in lithology and geochemistry studies.

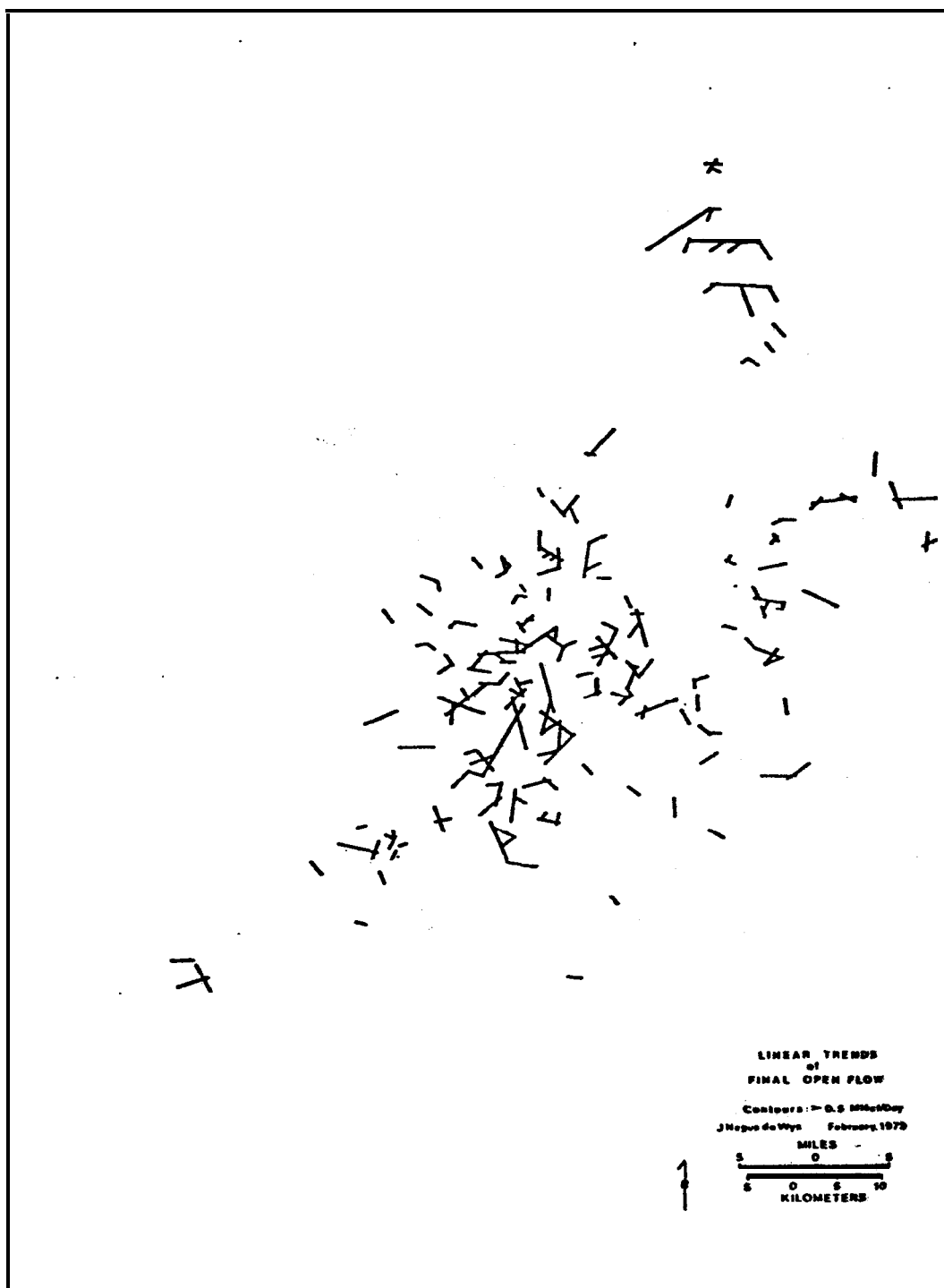


Figure 25. Trends of high open flow data taken from Figure 24.

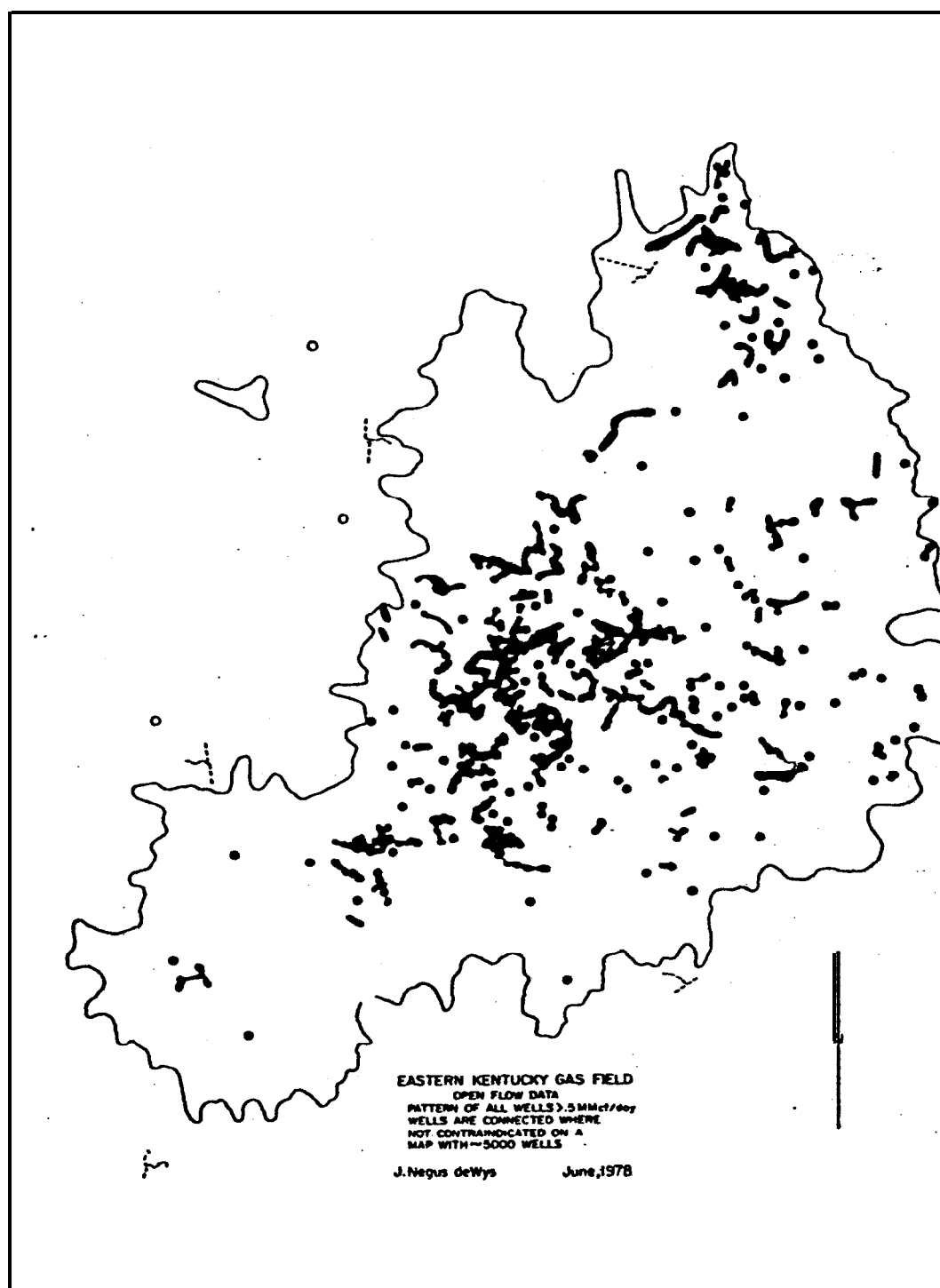


Figure 26. Pattern resulting from connecting all wells with $\geq .5$ MMcf/day where not contra indicated. This should be compared with Figure 20 in order to recognize the density of data and constraints of such density imposed on this pattern.

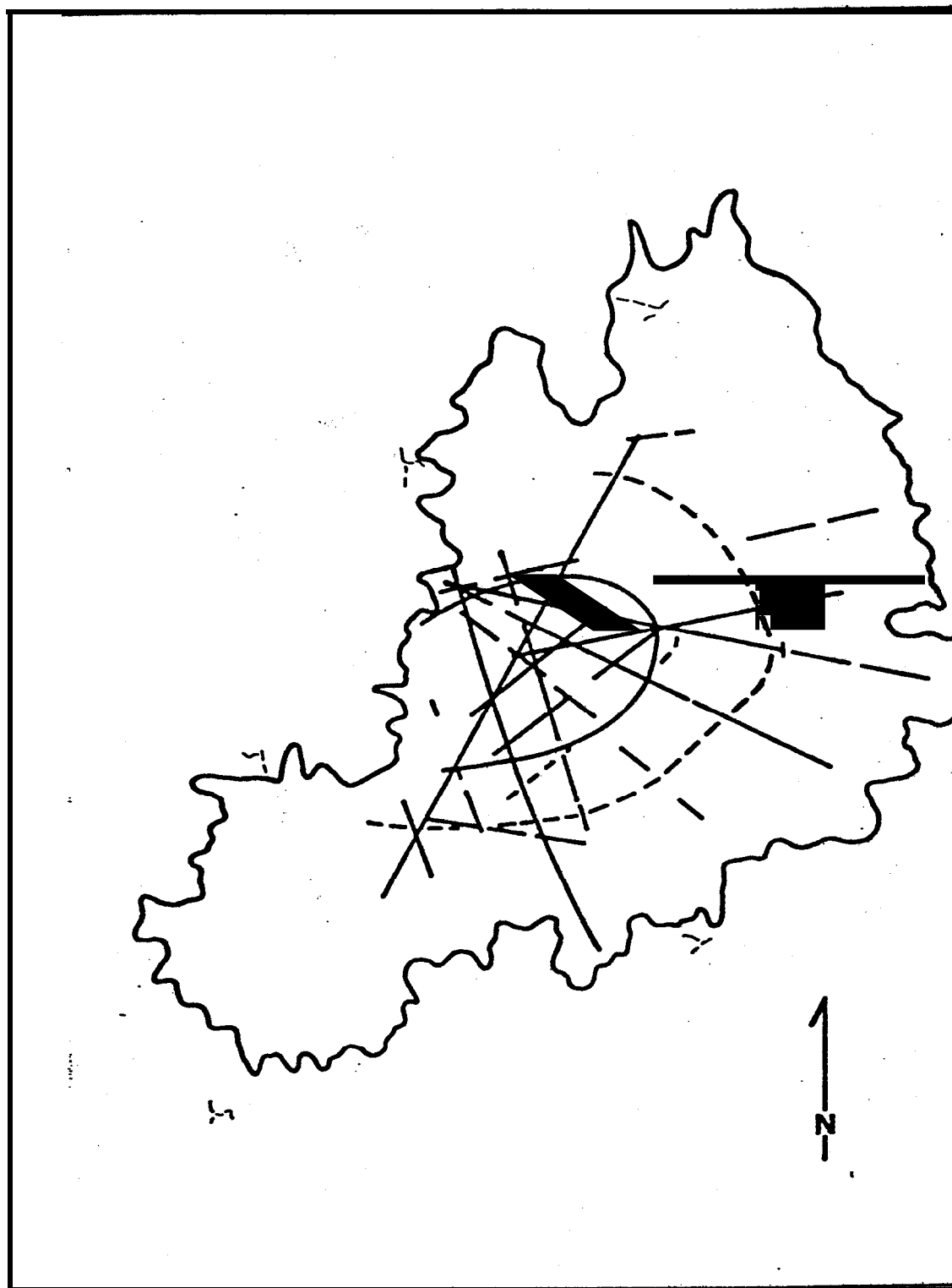


Figure 27. Pattern of open flow basic fracture band trends from Figure 26. Compare with Figures 6 and 16,

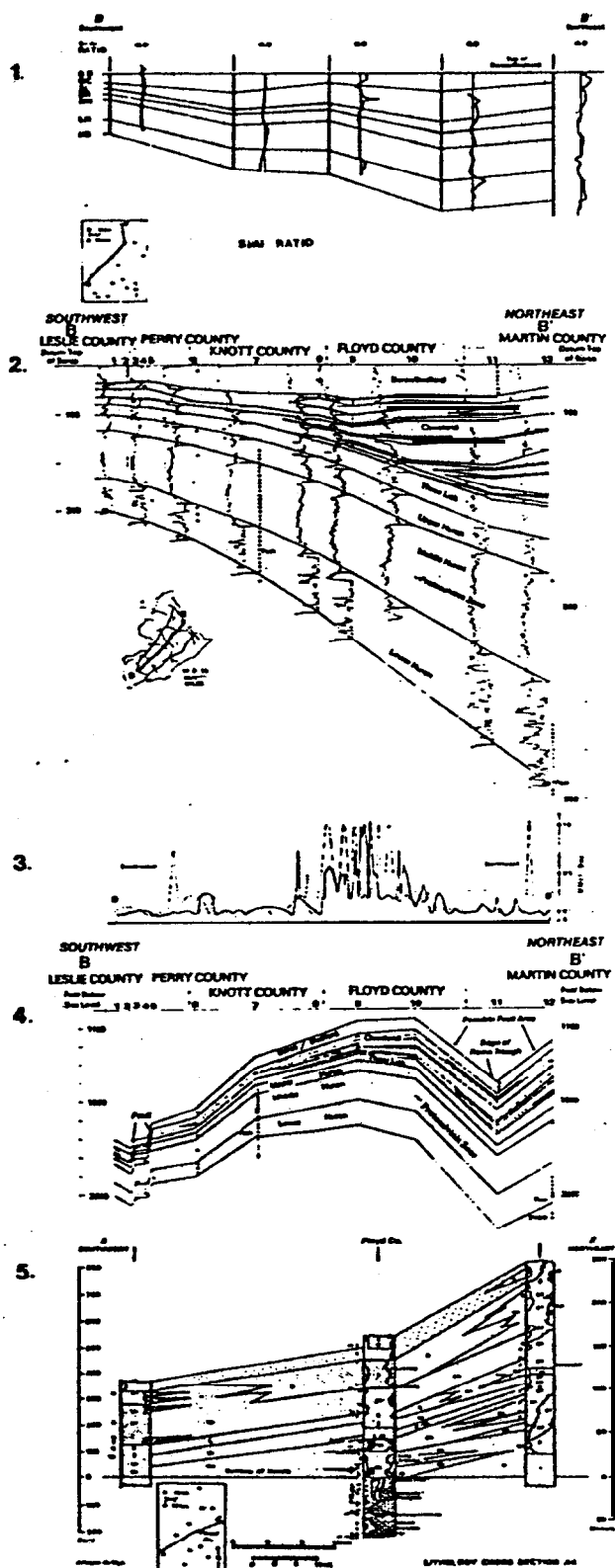


Figure 28. Comparison of similar cross sections.

References

- Bass, M. N., 1960, Grenville boundary in Ohio, *Journal of Geology*, Vol. 68, p. 673-677.
- Dever, G. R., Jr., H. P. Hoge, N. C. Hester, and F. R. Ettensohn, 1977, Stratigraphic evidence for late Paleozoic tectonism in northeastern Kentucky, Kentucky Geological Survey, University of Kentucky, Lexington, Ky., p. 78.
- Griffith, J., 1976, unpublished map and private communication.
- Hunter, C. D., and D. M. Young, 1953, Relationship of natural gas occurrences and production in eastern Kentucky (Big Sandy Gas Field) to joints and fractures in Devonian bituminous shales: *Bull. Am. Assoc. Pet. Geol.*, 37: 282-299.
- King, E. R. and I. Zietz, 1978, The New York-Alabama lineament: geophysical evidence for a major crustal break in the basement beneath the Appalachian basin, *Geology*, -Vol. 6, p. 312-318.
- Lafferty, R. C., 1941, Central basin of Appalachian Geosyncline, *Bulletin of Am. Assoc. Pet. Geol.*, Vol. 25, No. 5, p. 781-825.
- McFarlan, A. C., 1943, *Geology of Kentucky*, University of Kentucky, Lexington, Kentucky, p. 531.
- Muehleberger, W. R., R. E. Denison, and E. G. Lidiak, 1976, Basement rocks in continental interior of United States. *Bulletin of Am. Assoc. Pet. Geol.*, Vol. 51, p. 2351-2380.
- Negus-de Wys, Jane, 1979, The Eastern Kentucky Gas Field, Ph.D. Dissertation in Geology at West Virginia University, Morgantown, West-Virginia, and Final Report on DOE Contract No. DE-AC21-76-MC-05194, formerly EY-76-C-05-5194.
- Provo, L., 1977, Stratigraphy and sedimentology of radioactive Devonian-Mississippi shales of the central Appalachian Basin, Ph.D. Dissertation, University of Cincinnati, Cincinnati, Ohio, 128 p.
- Shumaker, R. C., 1977, Unpublished basement structure map from gravity from gravity data.
- Swager, D. R., 1978, Stratigraphy of the Upper Devonian-Lower Mississippian shale in the eastern Kentucky outcrop belts, Master's Thesis, University of Kentucky, Lexington, Kentucky, 116 p.